haematologica
Journal of the Ferrata Storti Foundation

Core regions in immunoglobulin heavy chain enhancers essential for survival of non-Hodgkin lymphoma cells are identified by a CRISPR interference screen

by Marta Elżbieta Kasprzyk, Weronika Sura, Marta Podralska, Marta Kazimierska, Annika Seitz, Wojciech Losiewski, Tomasz Woźniak, Jeroen E.J. Guikema, Arjan Diepstra, Joost Kluiver, Anke van den Berg, Natalia Rozwadowska, and Agnieszka Dzikiewicz-Krawczyk

Received: November 16, 2023.
Accepted: June 19, 2024.

Citation: Marta Elżbieta Kasprzyk, Weronika Sura, Marta Podralska, Marta Kazimierska, Annika Seitz, Wojciech Losiewski, Tomasz Woźniak, Jeroen E.J. Guikema, Arjan Diepstra, Joost Kluiver, Anke van den Berg, Natalia Rozwadowska, and Agnieszka Dzikiewicz-Krawczyk. Core regions in immunoglobulin heavy chain enhancers essential for survival of non-Hodgkin lymphoma cells are identified by a CRISPR interference screen. Haematologica. 2024 June 27. doi: 10.3324/haematol.2023.284672 [Epub ahead of print]

Core regions in immunoglobulin heavy chain enhancers essential for survival of non-Hodgkin lymphoma cells are identified by a CRISPR interference screen

Marta Elżbieta Kasprzyk[1*], Weronika Sura[1*], Marta Podralska[1], Marta Kazimierska[1], Annika Seitz[2], Wojciech Łosiewski[1], Tomasz Woźniak[1], Jeroen E. J. Guikema[3], Arjan Diepstra[2], Joost Kluiver[2], Anke van den Berg[2], Natalia Rozwadowska[1], Agnieszka Dzikiewicz-Krawczyk[1+]

[1] Institute of Human Genetics, Polish Academy of Sciences, Poznań, Poland
[2] Department of Pathology and Medical Biology, University of Groningen, University Medical Center Groningen, Groningen, The Netherlands
[3] Department of Pathology, Amsterdam University Medical Center, Amsterdam, The Netherlands

* Authors contributed equally

[+] Corresponding author. E-mail address: Agnieszka Dzikiewicz-Krawczyk agnieszka.dzikiewicz-krawczyk@igcz.poznan.pl. Postal address: Strzeszynska 32, 60-479 Poznan, Poland.

Funding

This research was carried out within the First Team programme of the Foundation for Polish Science co-financed by the European Union under the European Regional Development Fund (grant no. POIR.04.04.00-00-5EC2/18-00) and PROM programme, The Polish National Agency for Academic Exchange (NAWA) no. 10 PPI/PRO/2019/1/00014/U/00001 co-financed by the European Union under the European Social Fund. AD-K, NR and AvdB were supported by the European Union's Horizon 2020 research and innovation programme under grant agreement No 952304.

Authors contribution

MEK, WS: Investigation, Data analysis, Writing, Figure and table preparation; MP, MK, WŁ, AS: Investigation; TW: Data analysis; JEJG, AD, JK, AvdB, NR: Project conceptualization, providing materials and samples; ADK: Project conceptualization, Supervision, Funding acquisition, Project administration, Data analysis, Writing. All authors read and approved the manuscript.

Data availability

Raw and processed RNA-seq data have been deposited in Gene Expression Omnibus (GSE247393).

Declaration of competing interest

None of the authors have a conflict of interest.

Acknowledgements

The authors would like to thank prof. Reiner Siebert from Institute of Human Genetics, Ulm University for kindly providing BL2, BL60, JI and LY91 cell lines; dr. Natalia Derebecka from Laboratory of High Throughput Technologies, Institute of Molecular Biology and Biotechnology, Adam Mickiewicz University, Poznań, Poland for performing MiSeq analysis and dr. Wojciech Juzwa from Department of Biotechnology and Food Microbiology, Faculty of Food Science and Nutrition, Poznań University of Life Sciences for cell sorting of DG75-dCas9-EV cell line. Graphics for Figure 1E and Figure 5A were created with BioRender.

Abstract

Chromosomal translocations in non-Hodgkin lymphoma (NHL) result in activation of oncogenes by placing them under the regulation of immunoglobulin heavy chain (IGH) super-enhancers. Aberrant expression of translocated oncogenes induced by enhancer activity can contribute to lymphomagenesis. The role of the *IGH* enhancers in normal B-cell development is well established, but knowledge regarding the precise mechanisms of their involvement in control of the translocated oncogenes is limited. The goal of this project was to define the critical regions in the *IGH* regulatory elements and identify enhancer RNAs (eRNA). We designed a sgRNA library densely covering the *IGH* enhancers and performed tiling CRISPR interference screens in three NHL cell lines. This revealed three regions crucial for NHL cell growth. With chromatin-enriched RNA-Seq we showed transcription from the core enhancer regions and subsequently validated expression of the eRNAs in a panel of NHL cell lines and tissue samples. Inhibition of the essential *IGH* enhancer regions decreased expression of eRNAs and translocated oncogenes in several NHL cell lines. The observed expression and growth patterns were consistent with the breakpoints in the *IGH* locus. Moreover, targeting the Eμ enhancer resulted in loss of B-cell receptor expression. In a Burkitt lymphoma cell line, MYC overexpression partially rescued the phenotype induced by *IGH* enhancer inhibition. Our results indicated the most critical regions in the *IGH* enhancers and provided new insights into the current understanding of the role of *IGH* enhancers in B-cell NHL. As such, this study forms a basis for development of potential therapeutic approaches.

Keywords: IGH, enhancer, lymphoma, CRISPR/Cas9, BCR, MYC, BCL2

Introduction

Non-Hodgkin lymphomas (NHL) account for 3% of all cancer cases worldwide[1,2]. They arise from B cells at various stages of maturation, which is a multistep process involving several rearrangements occurring at the immunoglobulin heavy chain (IGH) locus. Obligatory intermediates during rearrangement of the *IGH* locus are DNA-double strand breaks. These breaks can result in illegitimate recombination and various chromosomal translocations including the t(8;14)(q24;q32) *MYC/IGH* in Burkitt lymphoma (BL) and t(14;18)(q32;q21) *IGH/BCL2* in diffuse large B-cell lymphoma (DLBCL) and follicular lymphoma[3]. As a result, the translocated oncogene is placed under the control of *IGH* enhancers, which leads to its overexpression. MYC is a transcription factor involved in many processes such as proliferation, apoptosis, DNA-damage response[4]. BCL2 suppresses cell death by preventing the activation of caspases which contributes to treatment resistance and poor prognosis[5]. Interestingly, oncogenic translocation itself may not be sufficient to drive lymphomagenesis[6], yet can contribute to instability that can in turn lead to accumulation of other mutations and malignant transformation[7]. The activity of the *IGH* locus is governed by enhancers: Eμ (the intronic enhancer) and 3' regulatory regions (3'RR1 and 3'RR2, Figure 1A)[8]. Among others, the feature of active enhancers is expression of enhancer RNAs (eRNAs). This class of non-coding RNAs was regarded as a by-product of an active transcription machinery, but increasing evidence shows that eRNAs can be functional[9]. Active transcription of 3'RR in activated B cells was first demonstrated by Peron et al[10]. Recently, the eRNA ARIEL was found to be a driver of oncogenesis in T-cell acute lymphoblastic leukemia[11]. In BL, the eRNA AL928768.3, expressed from 3'RR1, was shown to downregulate MYC expression upon knockdown[12]. Nevertheless, knowledge regarding the role of eRNAs in NHL remains limited.

The function of *IGH* enhancers has been extensively studied in normal B-cells. These studies showed that Eμ is important for earlier stages of B-cell development, mainly VDJ recombination[13], while 3'RR takes over the locus control at later stages, namely SHM and CSR[14]. Several mouse models demonstrated the involvement of *IGH* enhancers in regulation of oncogene expression and lymphomagenesis, but still more research is necessary to understand these processes in malignant human B-cells, where the *IGH* enhancers organization differs from mouse[15]. As *IGH* enhancers encompass a region of approximately 64 kb in total, it is important to pinpoint the core regions crucial for lymphoma cells.

The CRISPR/Cas9 system can be applied to study tissue-specific *cis*-regulatory elements of enhancers[16]. Here, we employed tiling CRISPR/dCas9-KRAB screen to pinpoint the critical regions within Eμ and 3'RRs in BL and DLBCL cell lines. RNA-seq of chromatin-enriched RNAs revealed transcriptional activity of *IGH* enhancers, which we also confirmed in primary patient samples. Further validation in several NHL cell lines revealed various patterns of dependency on *IGH* enhancers reflecting the differences in breakpoint location. The underlying molecular mechanisms involved disturbed expression of translocated oncogenes and is some cases also B-cell receptor (BCR) presentation.

Methods

Cell lines

Burkitt lymphoma: BL41, CA46, DG75 (DSMZ, Braunschweig, Germany), ST486 (ATCC, LGC Standards, Lomianki, Poland), BL2, BL60, JI, LY19 (gift from prof. Reiner Siebert, Ulm University, Germany), diffuse large B-cell lymphoma: SUDHL4, WSU-DLCL2 (DSMZ) and P493-6[17] (gift from prof. D. Eick, Helmholtz Center, Munich, Germany) were grown in RPMI 1640 (Lonza, Basel, Switzerland) and HEK293T (DSMZ) in DMEM (Lonza), supplemented with 2mM L-glutamine, 1% Penicillin-Streptomycin (Biowest, Nuaillé, France) and 10-20% fetal bovine serum (Sigma-Aldrich, Saint Louis, MO, USA). Standard conditions: 37°C, 5% CO_2, humidified incubator. Cells were regularly tested for *Mycoplasma* contamination by PCR.

Patient samples

Enhancer RNA expression was validated in patient-derived NHL samples: BL (8 cases, all MYC translocation positive) and DLBCL (14 cases: 6 germinal center B-cell (GCB), 7 activated B-cell (ABC) and 1 unclassfied) as well as tonsil tissues obtained during tonsillectomy as controls (6 cases). Tissues were obtained from the Pathology files of the University Medical Center Groningen tissue bank. They were used in accordance with the Declaration of Helsinki and the protocol was approved by the Medical Ethical Review board of the UMCG (RR#201800554).

Design and generation of the CRISPR-eIGH library

IGH enhancer regions were defined by the H3K27ac plus 5 kb flanking sequences (hg19): Eμ (chr14:106317800-106336124), 3'RR1 (chr14:106140100-106181250) and 3'RR2 (chr14:106019800-106055011). Tiling library of sgRNAs covering those regions was designed and cloned into the lentiGuide-Puro vector[18].

CRISPR screen

27.5 x 10^6 cells stably expressing dCas9-KRAB were transduced in duplicate with CRISPR-eIGH library, with the previously established amount of virus. After four days of selection with puromycin (T0) 8 x 10^6 cells were collected for DNA isolation. Remaining cells were further cultured for 20 population doublings. At each passage, the number of cells corresponding to 1,000x coverage of the library, that is 8 x 10^6, were cultured in RPMI medium with 1 µg/ml (DG75) or 0.3 µg/ml (other cell lines) puromycin and collected at the final timepoint (T1).

Chromatin-enriched RNA-Seq and data analysis

RNA from chromatin fraction was sent for RNA-Seq stranded library preparation, pair-end sequencing and bioinformatic data analysis to Novogene (Beijing, China). Sequencing was performed on Illumina X-Ten platform. Quality control of raw data in FASTQ format was performed, clean data were obtained by removing reads containing adapter and poly-N sequences and reads with low quality. Approximately 77-92 x 10^6 clean reads were obtained per sample. All downstream analyses were based on clean data with high quality. Reads were mapped to the human reference genome version GRCh37.87 using HISAT 2 software. Reads mapping to the *IGH* enhancer regions (see **Design of the CRISPR-eIGH library**) were selected for further study. Using Galaxy[19] BAM files provided by Novogene were sliced by genomic region chr14:106019800-106337000 and filtered by second mate to retrieve information about the strand from which the transcript was derived. Next, using Integrative Genome Browser[20], BedGraph files were generated and visualized in UCSC Genome Browser (http://genome.ucsc.edu)[21].

Results

Generation of the CRISPR-eIGH library targeting *IGH* enhancers

Target regions of the human Eµ, 3'RR1 and 3'RR2 were defined by the H3K27ac histone mark in B cells (GM12878 cell line from ENCODE) (Supplementary Figure 1) and a total of 18,732 sgRNAs were designed. Due to homology within the 3'RR1 and 3'RR2 regions, several sgRNAs were present multiple times in the design and sgRNAs targeting up to two sites within the regions of interest were allowed (12,062 sgRNAs remained). Further testing for off-targets elsewhere in the genome excluded 5,080 sgRNAs. The final library included 6,982 sgRNAs that cover the Eµ and 3'RR with an average distance

between the sgRNAs of 8 bp for the Eμ and 11 bp for 3'RRs (Figure 1B). 2,344 sgRNAs were common for 3'RR1 and 3'RR2. Including the negative and positive control sgRNAs, the final library consisted of 7,971 sgRNAs (Supplementary Table 1).

NGS-based quality control of the CRISPR-eIGH library confirmed its completeness and integrity (Figure 1C). 88.6% of guides matched perfectly and there were no undetected guides. The skew ratio of top 10% to bottom 10% was 1.58. This confirms good quality of the generated CRISPR-eIGH library.

CRISPRi screen identifies elements of *IGH* enhancers essential for lymphoma cell growth

To identify essential elements of the *IGH* enhancers, we performed a CRISPR interference screen. (Figure 1D). First, we generated lymphoma cell lines (BL41, DG75, SUDHL4) stably expressing the catalytically inactive Cas9 fused with the repressive KRAB domain (dCas9-KRAB) (Supplementary Figure 2A). These cells were thereafter transduced in duplicate with lentivirus carrying the CRISPR-eIGH library. We achieved transduction efficiency between 21.8% and 30.4% and the coverage of 750x-1,045x (Supplementary Figure 2B). Cells were collected at T0 (after puromycin selection) and at T1 (after 20 population doublings) and the abundance of sgRNA constructs was assessed using NGS. In each cell line we identified a few hundreds of sgRNA constructs showing a consistent ≥ 2-fold depletion in both screen replicates (Figure 2A, Supplementary Table 2). Non-targeting sgRNAs did not show any major effects, while several sgRNAs targeting CD79a and CD79b were depleted as expected.

Using a sliding window approach we identified three essential regions, hereafter called peaks, marked by sgRNAs highly depleted over time (Supplementary Table 3): one Eμ-peak and two peaks in each of 3'RRs: 3'RR-peak1 and 3'RR-peak2 (Figure 2B). The profoundness of depletion varied between cell lines. For the Eμ-peak the strongest effect was observed in SUDHL4, with log2 FC values reaching -1.4, followed by DG75 (log2 FC -0.8), while in BL41 it did not exceed -0.4. In both 3'RR peaks we observed the strongest effect in DG75 (log2 FC ~-2), while BL41 and SUDHL4 showed less depletion (log2 FC ~-1). The significant peaks within 3'RRs overlapped with known DNase I hypersensitive sites (HS) HS4 and HS1.2.

We selected two sgRNAs per peak to validate the effect on cell growth in a GFP competition assay in a larger set of BL and DLBCL cell lines. In line with the results of the screen, we observed progressive depletion of BL and DLBCL cells transduced with sgRNA constructs targeting enhancer-essential regions compared to non-targeting controls (Figure 2C-D). The dependency of B-cells on *IGH* enhancers varied between cell lines, which is possibly linked to differences in the location of the

breakpoints in *IGH* (Figure 2E). In DG75[22], SUDHL4 and WSU-DLCL2[23] the breakpoint occurs in V/D/J region, hence the Eμ is involved in the translocation. Accordingly, the strongest effect on survival in SUDHL4 and WSU-DLCL2 was observed upon inhibition of the Eμ-peak, while DG75 was very susceptible to blocking of all identified essential *IGH* regions. BL41 and CA46 have a breakpoint within the constant region Cα1[22] resulting in Eμ exclusion from the *IGH* locus on the translocated allele, and the strongest effect on survival in those cells was observed upon blocking of 3'RR-peak1, followed by 3'RR-peak2 and Eμ. ST486 cell line with breakpoint within the switch region μ[24] proved to be the most resistant to blocking of core *IGH* enhancers regions.

Altogether, our CRISPRi screens identified specific regions in the *IGH* enhancers, essential for survival of B-cell lymphoma cells.

Chromatin-enriched RNA-Seq reveals enhancer RNA transcripts from *IGH* enhancers

To identify transcription of eRNAs from the *IGH* locus, we performed cellular fractionation combined with chromatin-enriched RNA-Seq in BL41, DG75, SUDHL4 lymphoma cells and P493-6 along with HEK239T as controls (no IGH translocation). This method allows for relatively fast, reproducible and cost-effective enrichment of eRNAs (Supplementary Figure 3A). Proper fractionation was confirmed by RNA agarose gel electrophoresis (Supplementary Figure 3B), and by using appropriate markers on RNA and protein levels (Supplementary Figure 3C-D).

Focusing on transcripts mapping to the *IGH* enhancers, we observed bidirectional transcription from the Eμ and 3'RRs (Figure 3A, Supplementary Figures 4-5) in B-lineage cell lines, but not in HEK293T. The significant peaks identified in the CRISPRi screen were also transcriptionally active. In the Eμ transcription from the minus strand was 10-fold higher compared to the plus strand, with the highest read counts for BL cell lines. In 3'RR1 transcription rates were comparable from both strands. For the 3'RR2 more reads were mapped to the plus strand especially for BL41 and SUDHL4.

Cellular localization of eRNAs transcribed from core *IGH* enhancers regions was confirmed with RT-qPCR in subcellular fractions (Figure 3B). eRNAs from the Eμ-peak and 3'RR-peak2 were enriched in the chromatin, while the 3'RR-peak1 eRNA was enriched in the cytoplasm.

***IGH*-eRNAs expression in B-cell lymphoma cell lines and patient-derived samples**

We verified eRNA expression from the essential *IGH* regions in a panel of B-cell lymphoma cell lines (Figure 3C). We observed statistically significant lower expression of all tested eRNAs in Hodgkin lymphoma cell lines. There were no differences in expression levels between other groups, including ABC

and GCB type DLBCLs. In line with NGS results, we observed higher expression from the Eμ-peak compared to 3'RR-peaks.

Next we confirmed eRNA expression in patient-derived FFPE samples (Figure 3D), including 8 BL and 13 DLBCL, and 6 tonsils as control. We observed statistically significant higher expression of 3'RRs in BL.

Downstream effects of targeting *IGH* enhancers on the expression of eRNAs, translocated oncogenes and B-cell receptor

Next we determined the effects of inhibition of significant *IGH* peaks on expression of eRNAs, translocated oncogenes and BCR. Targeting of *IGH* enhancers peaks with selected sgRNAs significantly downregulated expression of eRNAs from the respective regions (Figure 4A, Supplementary Figure 6A). In the BL cell lines BL41 and DG75 blocking of each *IGH* peak led to a consistent, up to 50% decrease of MYC transcript level. This was accompanied by reduced protein levels in DG75 (Supplementary Figure 7). In the BL cell line CA46 downregulation of MYC transcript was observed only upon blocking of 3'RRs, but not Eμ (Supplementary Figure 6A), while the MYC protein was consistently decreased in all samples (Supplementary Figure 7). ST486, which in GFP assay appeared to be more resistant, did not exhibit downregulation of MYC, neither on RNA nor protein level (Supplementary Figure 6A, Supplementary Figure 7). In DLBCL cell lines SUDHL4 and WSU-DLCL2 BCL2 expression was decreased on both RNA and protein levels in nearly all samples (Figure 4A, Supplementary Figure 6A, Supplementary Figure 7).

Usually, one *IGH* allele is involved in the translocation, while the other allele is productively rearranged and leads to production of secreted immunoglobulins and expression of the BCR on the cell surface (IgM or IgG)[25]. Throughout their lifetime B-cells, including lymphoma cells, are constantly tested for proper BCR presentation on cell surface[25] as their development and survival depend on it. Our CRISPRi approach targets both the translocated and functional *IGH* alleles. Thus, we checked whether silencing *IGH* enhancers with dCas9-KRAB also leads to changes in BCR expression (Supplementary Figure 8). Targeting of the Eμ-peak resulted in appearance of an IgM-negative population in BL cell lines BL41 (50% IgM(-)), DG75 (up to 30% IgM(-)) (Figure 4B-C), CA46 (70% IgM(-)), but not in ST486 (Supplementary Figure 6B-C). A similar effect was observed in IgG-expressing DLBCL cell line SUDHL4 with a BCR-negative population reaching 30-40% (Figure 4B-C). In contrast to the Eμ-peak, targeting of the 3'RR-peaks led only to a slight reduction in BCR expression in SUDHL4, but not in the other cell lines (Figure 4B-C and Supplementary Figure 6B-C).

IGH enhancers are active only in B cells. Therefore, no effect should be observed upon targeting them in non-B cells. In addition, based on the results of BCR expression, we expected that our CRISPRi approach would affect growth of B cells without IGH translocations only if they depended on BCR signaling and the Eμ enhancer was targeted. To test this, we assessed cell growth and BCR expression in 1) BL cell lines with MYC-IGL t(8;22) translocation (BL2, BL60); 2) BL cell lines with MYC-IGK t(2;8) translocation (JI, LY91); 3) B-cell cell line without MYC translocation (P493-6); 4) embryonic kidney HEK293T cell line. We observed reduced cell growth in BL2, BL60 and P493-6 cells transduced with sgRNA targeting the Eμ peak. JI and LY91 cells did not respond to any construct, neither did HEK293T cells where IGH enhancers not active (Supplementary Figure 9A-D). In line with this, JI and LY91 cells are BCR-negative, they do not express neither IgM nor IgG (data not shown). BL2, BL60 and P493-6 cells express surface IgM and we observed a 20-30% (BL2), 40-70% (BL60) and 82-85% (P493-6) decrease in IgM-positive cells upon targeting the Eμ peak (Supplementary Figure 9E). This confirmed that while the effect of silencing the Eμ enhancer may be attributed to interfering with both the oncogene expression and BCR, reduced cell growth observed upon 3'RR targeting is not related to the BCR signaling.

MYC overexpression rescues cell proliferation in Burkitt lymphoma cell line upon *IGH* enhancer inhibition

Since we observed a significant decrease in cell growth accompanied by MYC downregulation in DG75 upon blocking of *IGH* enhancers, we determined whether MYC overexpression could rescue the phenotype (Figure 5A). To this end we generated a DG75 cell line with a doxycycline-inducible MYC expression (DG75-MYC-OE, Supplementary Figure 10A). As control, cells with empty vector (DG75-EV) were used. Induction of MYC expression was tested on both RNA and protein level (Supplementary Figure 10B-C) with doxycycline doses 0.1-0.5 μg/ml. Survival of DG75-MYC-OE cells upon induction of MYC expression was determined over a course of 3 weeks (Supplementary Figure 10D). We established that the use of 0.1 μg/ml is sufficient for MYC overexpression, while higher doses caused a strong decrease in cell survival. Next, DG75-MYC-OE and DG75-MYC-EV cells were transduced with the set of sgRNAs targeting *IGH* enhancers peaks and non-targeting controls and their viability was tested. We observed a partial rescue of the effect exerted by inhibition of *IGH* enhancers in DG75-MYC-OE cells upon MYC induction (Figure 5B), but not in DG75-EV (Figure 5C). Although we could not fully rescue the observed effects on viability upon targeting IGH enhancers, our results suggest that the observed negative effect is at least in part caused by downregulation of MYC.

Discussion

In NHL, recurrent chromosomal translocations are known to bring oncogenes under the regulation of *IGH* enhancers – 5' intronic Eμ and 3'regulatory regions, 3'RR1 and 3'RR2. Up to date, targeting the *IGH* enhancers as therapeutic options remains elusive. Therefore, delineation of the core *IGH* enhancers regions, which control the expression of translocated oncogenes, as well as growth and survival of lymphoma cells is of a key importance. Our study is the first to define the exact regions crucial for survival of NHL. The use of a saturating CRISPRi library allowed us to target and thoroughly screen the *IGH* enhancers. Interestingly, survival of lymphoma cells upon blocking of *IGH* enhancers core regions varied between cell lines. Taking into account that chromosomal translocations can occur at various regions within the *IGH* locus, our data suggest that the observed patterns are connected to the breakpoint sites.

In DG75, SUDHL4 and WSU-DLCL2 both the Eμ enhancer and 3'RRs are involved in the translocation. We observed consistent downregulation of the translocated oncogene (MYC or BCL2) upon blocking *IGH* enhancers, with a similar effect for each of the identified essential regions. This may indicate a cooperation between *IGH* enhancers in driving expression of the translocated oncogene. Spatial interaction between Eμ and 3'RR occurs for example during *IGH* locus rearrangements[26]. Ghazzaui et al.[27] developed several mouse models of c-myc knock-in juxtaposed with *IGH* enhancers and demonstrated that the dynamics of lymphoma development and mice survival varied, depending on the oncogene insertion site. The shortest lifespan was observed when both Eμ and 3'RR enhancers were involved. They concluded that Eμ and 3RR enhancers cooperate in driving translocated oncogenes expression and lymphomagenesis. We tested in our study whether inhibition of one core *IGH* enhancer region affects transcription of others, but we did not observe any consistent effect on eRNAs expression from 3'RR when blocking Eμ and *vice versa* (data not shown).

In BL cell lines BL41, CA46 and ST486 the intronic Eμ is not involved in the translocation with MYC. In agreement with this, we observed little to no MYC downregulation upon targeting of the Eμ enhancer essential region. In contrast, blocking of 3'RRs core regions in BL41 and CA46 had a significant effect on MYC transcript levels as well as cell survival. In NHLs, despite differences in the location of the breakpoint in *IGH*, the 3'RR always remains in the *IGH* locus. This regulatory region was suggested previously to be a good target for therapy[28,29] and was found sufficient to deregulate oncogene expression[7,27]. So far, several factors were shown to affect transcriptional activity of 3'RR, proving that this enhancer may be druggable[30–32]. The 3'RRs span 25-30 kb each, therefore it is necessary to further

pinpoint which sites to target. In mice, HS3a and HS1.2 were shown to be important for deregulation of the translocated MYC[33]. Our approach revealed HS4 (peak1) and HS1.2 (peak2) within 3'RRs as crucial for human B-cell lymphoma cells survival. Importantly, P493-6 cell line was not affected by blocking of 3'RRs, in contrast to Eμ. This suggests that the 3'RR-peaks identified by us are attractive candidates for therapeutic targeting. However, it still needs to be determined whether inhibition of HS4 and HS1.2 is toxic specifically for *IGH*-translocation positive lymphomas and not for normal B cells.

ST486 cells exhibited resistance to inhibition of *IGH* core enhancers regions. This cell line bears several translocations involving MYC: typical BL reciprocal translocation MYC/IGH t(8;14)(q24;q32) but also complex t(8;14;18)(q24;q32;q23)[34]. This leads to the presence of MYC at as many as four different locations: chromosome 8, der(8), der(14) and der(18). Probably downregulation of MYC expression from only one site was not enough to observe a significant change in overall levels, nor a more profound effect on cell proliferation.

We were able to partially rescue the phenotype of blocking *IGH* enhancers by MYC overexpression in a BL cell line. This suggests that other elements controlled by *IGH* enhancers may be involved. Most lymphoma cells retain expression of BCR from the non-translocated *IGH* allele. In our approach, sgRNAs for *IGH* enhancer-essential regions can target both alleles. We observed partial BCR loss upon blocking of the Eμ-peak in nearly all tested lymphoma cell lines with IGH translocations but also in BL cells with IGL translocations and in P493-6 B cell line which does not harbor any IG translocation. In contrast, targeting 3'RR-peaks in general did not affect BCR expression. This is in line with previous studies showing a reduction of IgM and IgG expressing B cells in mice with deletion of the Eμ enhancer[8,35–37]. On the other hand, singular deletions of 3'RR enhancer components in mice were not sufficient[38–41] and only combinatorial deletion of HS4 and HS3b downregulated BCR in B-cells[42,43]. However, other studies showed that deletion of HS3b and HS4 or even the whole 3'RR did not affect surface IgM, only IgG was reduced[29,44–46]. Interestingly, it has been shown that while BCR ablation per se does not negatively influence lymphoma growth, BCR-negative BL cells are outcompeted by their BCR-expressing counterparts[47]. This is similar to the effect on cell survival observed by us upon Eμ-peak inhibition in the GFP-growth competition assays. Taken together, our results indicate that the reduced cell growth observed upon inhibition of essential *IGH* enhancer regions can be attributed to downregulation of oncogene expression and in case of the Eμ – also to the loss of BCR.

Current knowledge regarding the function of eRNAs in NHL is very limited. Recently, a B-cell specific eRNA AL928768.3 was shown to regulate MYC expression in BL[12]. This eRNA resides within human 3'RR1 region (hg19, chr14:106170301-10617093). Authors modulated the expression of

AL928768.3 by either siRNA-mediated knock-down or overexpression, and observed down- and upregulation of MYC, respectively. The effect on MYC was specific to cells bearing *MYC/IGH* translocation. Knock-down of eRNA AL928768.3 resulted in a decrease in BL cell proliferation. Verification of this observation in a wider panel of NHL would be of interest. In our screen, inhibition of AL928768.3 region with CRISPR/dCas9 had in general no significant impact on cell survival overall; however a few individual sgRNAs were strongly depleted, especially in DG75 and SUDHL4 (Supplementary Table 6). Here, we confirmed transcription from core *IGH* enhancers regions and validated arising eRNAs in a panel of B-cell lymphomas, both NHL and HL, as well as NHL patient-derived samples. It was shown that the activity of IGH enhancers depends on transcription factors such as e.g. BOB.1 and PU.1[48]. Low expression of IGH eRNAs in HL is in line with absence of those transcription factors[48,49]. Levels of BOB.1 and PU.1 are high in BL and germinal center B cells but variable in DLBCL[48,49], which may account for the observed differences.

Blocking transcription of the essential regions with CRISPRi resulted in downregulation of eRNAs derived from them, which was accompanied by oncogene and BCR downregulation. Whether *IGH* eRNAs from core regions are indeed involved in the regulation of those translocated oncogenes and BCR requires further study. For some eRNAs the very act of their transcription and not necessarily the transcript itself is important for carrying out their function[9,50]. On the other hand, enhancer RNAs may help achieve proper chromatin conformation and recruit transcriptional machinery to target regions[51]. Transcription of 3'RR in mice was shown to recruit activation-induced cytidine deaminase, which leads to *IGH* locus suicide recombination and BCR loss, potentially contributing to B-cell homeostasis[10]. eRNAs can also interact with other classes of non-coding RNAs. Long non-coding RNA CSR (lncRNA-CSR) interacts with 3'RR's HS4 eRNA, which promotes CSR[52]. Apart from these functions in chromatin, the role of eRNAs in the cytoplasm has also been reported[53]. We observed a predominant cytoplasmic localization of the eRNA from 3'RR-peak 1 which suggest that it may have additional role beyond acting *in cis* in the IGH locus. So far, we were not able to efficiently knock down *IGH* eRNAs with the use of either Gapmers or shRNAs, therefore the potential role of *IGH* eRNAs requires further investigation.

A more detailed analysis of the *IGH* enhancers core regions would be of interest. Enhancers are known to be packed with transcription factors binding sites. Elucidation if and how their binding is affected upon blocking of essential enhancer sites will help understand expression regulation at those regions. In addition, Eμ and 3'RRs can form chromatin loops, so a closer look at the chromatin architecture in the *IGH* locus upon blocking of the core enhancer regions could provide insights into the mechanisms involved. Inhibition of the *IGH* enhancers allows for a precise, B-cell restricted, targeting of translocated oncogenes in B-cell lymphoma. This makes the core regions identified by us attractive

targets for therapeutic approaches. So far, HDAC inhibitors and aryl hydrocarbon receptor ligands have been shown to affect activity of the 3'RR and *IGH* transcription[30,31]. However, their effect on lymphomas driven by *IGH* translocations has not been evaluated. Recently, a small molecule reducing the activity of the Eμ has been reported, with an inhibitory effect on growth of *IGH* translocation positive multiple myeloma cells *in vitro* and *in vivo*[54]. However, we showed that this compound is also toxic to other cell types[32].

In summary, we pinpointed regions within *IGH* enhancers Eμ and 3'RR crucial for survival of B-cell lymphomas. We showed that the observed negative effect on cell survival is likely to be attributed to downregulation of translocated oncogenes and in case of Eμ inhibition also to BCR loss. Our results set a frame for further studies to explore the therapeutic potential of inhibiting *IGH* enhancers in B-cell lymphoma.

References

1. Thandra KC, Barsouk A, Saginala K, Padala SA, Barsouk A, Rawla P. Epidemiology of Non-Hodgkin's Lymphoma. Med Sci (Basel). 2021;9(1):5.

2. Sedeta E, Ilerhunmwuwa N, Wasifuddin M, et al. Epidemiology of Non-Hodgkin Lymphoma: Global Patterns of Incidence, Mortality, and Trends. Blood. 2022;140(Supplement 1):5234-5235.

3. Küppers R, Dalla-Favera R. Mechanisms of chromosomal translocations in B cell lymphomas. Oncogene. 2001;20(40):5580-5594.

4. Ahmadi SE, Rahimi S, Zarandi B, Chegeni R, Safa M. MYC: a multipurpose oncogene with prognostic and therapeutic implications in blood malignancies. J Hematol Oncol. 2021;14(1):121.

5. Klanova M, Klener P. BCL-2 Proteins in Pathogenesis and Therapy of B-Cell Non-Hodgkin Lymphomas. Cancers (Basel). 2020;12(4):938.

6. Brassesco MS. Leukemia/lymphoma-associated gene fusions in normal individuals. Genet Mol Res. 2008;7(3):782-790.

7. Ferrad M, Ghazzaui N, Issaoui H, Cook-Moreau J, Denizot Y. Mouse Models of c-myc Deregulation Driven by IgH Locus Enhancers as Models of B-Cell Lymphomagenesis. Front Immunol. 2020;11:1564.

8. Saintamand A, Vincent-Fabert C, Marquet M, et al. Eμ and 3'RR IgH enhancers show hierarchic unilateral dependence in mature B-cells. Sci Rep. 2017;7(1):442.

9. Han Z, Li W. Enhancer RNA: What we know and what we can achieve. Cell Prolif. 2022;55(4):e13202.

10. Péron S, Laffleur B, Denis-Lagache N, et al. AID-driven deletion causes immunoglobulin heavy chain locus suicide recombination in B cells. Science. 2012;336(6083):931-934.

11. Tan SH, Leong WZ, Ngoc PCT, et al. The enhancer RNA ARIEL activates the oncogenic transcriptional program in T-cell acute lymphoblastic leukemia. Blood. 2019;134(3):239-251.

12. Stasevich EM, Uvarova AN, Murashko MM, et al. Enhancer RNA AL928768.3 from the IGH Locus Regulates MYC Expression and Controls the Proliferation and Chemoresistance of Burkitt Lymphoma Cells with IGH/MYC Translocation. Int J Mol Sci. 2022;23(9):4624.

13. Afshar R, Pierce S, Bolland DJ, Corcoran A, Oltz EM. Regulation of IgH gene assembly: role of the intronic enhancer and 5'DQ52 region in targeting DHJH recombination. J Immunol. 2006;176(4):2439-2447.

14. Pinaud E, Marquet M, Fiancette R, et al. The IgH locus 3' regulatory region: pulling the strings from behind. Adv Immunol. 2011;110:27-70.

15. Kasprzyk ME, Sura W, Dzikiewicz-Krawczyk A. Enhancing B-Cell Malignancies-On Repurposing Enhancer Activity towards Cancer. Cancers (Basel). 2021;13(13):3270.

16. Li K, Liu Y, Cao H, et al. Interrogation of enhancer function by enhancer-targeting CRISPR epigenetic editing. Nat Commun. 2020;11(1):485.

17. Pajic A, Spitkovsky D, Christoph B, et al. Cell cycle activation by c-myc in a burkitt lymphoma model cell line. Int J Cancer. 2000;87(6):787-793.

18. Sanjana NE, Shalem O, Zhang F. Improved vectors and genome-wide libraries for CRISPR screening. Nat Methods. 2014;11(8):783-784.

19. Afgan E, Baker D, van den Beek M, et al. The Galaxy platform for accessible, reproducible and collaborative biomedical analyses: 2016 update. Nucleic Acids Res. 2016;44(W1):W3-W10.

20. Freese NH, Norris DC, Loraine AE. Integrated genome browser: visual analytics platform for genomics. Bioinformatics. 2016;32(14):2089-2095.

21. Kent WJ, Sugnet CW, Furey TS, et al. The Human Genome Browser at UCSC. Genome Res. 2002;12(6):996-1006.

22. Basso K, Frascella E, Zanesco L, Rosolen A. Improved long-distance polymerase chain reaction for the detection of t(8;14)(q24;q32) in Burkitt's lymphomas. Am J Pathol. 1999;155(5):1479-1485.

23. Chong LC, Ben-Neriah S, Slack GW, et al. High-resolution architecture and partner genes of MYC rearrangements in lymphoma with DLBCL morphology. Blood Adv. 2018 Oct 23;2(20):2755-2765.

24. Shiramizu B, Magrath I. Localization of breakpoints by polymerase chain reactions in Burkitt's lymphoma with 8;14 translocations. Blood. 1990;75(9):1848-1852.

25. Seda V, Mraz M. B-cell receptor signalling and its crosstalk with other pathways in normal and malignant cells. Eur J Haematol. 2015;94(3):193-205.

26. Ju Z, Volpi SA, Hassan R, et al. Evidence for physical interaction between the immunoglobulin heavy chain variable region and the 3' regulatory region. J Biol Chem. 2007;282(48):35169-35178.

27. Ghazzaui N, Issaoui H, Ferrad M, et al. Eμ and 3'RR transcriptional enhancers of the IgH locus cooperate to promote c-myc-induced mature B-cell lymphomas. Blood Adv. 2020;4(1):28-39.

28. Saintamand A, Saad F, Denizot Y. 3'RR targeting in lymphomagenesis: a promising strategy? Cell Cycle. 2015;14(6):789-790.

29. Saad F, Saintamand A, Rouaud P, Denizot Y. Targeting the oncogene B lymphoma deregulator IgH 3' regulatory region does not impede the in vivo inflammatory response in mice. Oncoscience. 2014;1(9):591-598.

30. Lu ZP, Ju ZL, Shi GY, Zhang JW, Sun J. Histone deacetylase inhibitor Trichostatin A reduces anti-DNA autoantibody production and represses IgH gene transcription. Biochem Biophys Res Commun. 2005;330(1):204-209.

31. Wourms MJ, Sulentic CE. The aryl hydrocarbon receptor regulates an essential transcriptional element in the immunoglobulin heavy chain gene. Cell Immunol. 2015;295(1):60-66.

32. Kasprzyk ME, Łosiewski W, Podralska M, Kazimierska M, Sura W, Dzikiewicz-Krawczyk A. 7-[[(4-methyl-2-pyridinyl)amino](2-pyridinyl)methyl]-8-quinolinol (compound 30666) inhibits enhancer

activity and reduces B-cell lymphoma growth - A question of specificity. Eur J Pharmacol. 2021;910:174505.

33. Kovalchuk AL, Sakai T, Qi CF, et al. 3'Igh enhancers hs3b/hs4 are dispensable for Myc deregulation in mouse plasmacytomas with T(12;15) translocations. Oncotarget. 2018;9(77):34528-34542.

34. Zimonjic DB, Keck-Waggoner C, Popescu NC. Novel genomic imbalances and chromosome translocations involving c-myc gene in Burkitt's lymphoma. Leukemia. 2001;15(10):1582-1588.

35. Peng C, Eckhardt LA. Role of the Igh intronic enhancer Eμ in clonal selection at the pre-B to immature B cell transition. J Immunol. 2013;191(8):4399-43411.

36. Marquet M, Garot A, Bender S, et al. The Eμ enhancer region influences H chain expression and B cell fate without impacting IgVH repertoire and immune response in vivo. J Immunol. 2014;193(3):1171-1183.

37. Saintamand A, Rouaud P, Garot A, et al. The IgH 3' regulatory region governs μ chain transcription in mature B lymphocytes and the B cell fate. Oncotarget. 2015;6(7):4845-4852.

38. Volpi SA, Verma-Gaur J, Hassan R, et al. Germline deletion of Igh 3' regulatory region elements hs 5, 6, 7 (hs5-7) affects B cell-specific regulation, rearrangement, and insulation of the Igh locus. J Immunol. 2012;188(6):2556-2566.

39. Bébin AG, Carrion C, Marquet M, et al. In vivo redundant function of the 3' IgH regulatory element HS3b in the mouse. J Immunol. 2010;184(7):3710-3717.

40. Manis JP, van der Stoep N, Tian M, et al. Class switching in B cells lacking 3' immunoglobulin heavy chain enhancers. J Exp Med. 1998;188(8):1421-1431.

41. Vincent-Fabert C, Truffinet V, Fiancette R, Cogné N, Cogné M, Denizot Y. Ig synthesis and class switching do not require the presence of the hs4 enhancer in the 3' IgH regulatory region. J Immunol. 2009;182(11):6926-6932.

42. Garot A, Marquet M, Saintamand A, et al. Sequential activation and distinct functions for distal and proximal modules within the IgH 3' regulatory region. Proc Natl Acad Sci U S A. 2016;113(6):1618-1623.

43. Pinaud E, Khamlichi AA, Le Morvan C, et al. Localization of the 3' IgH locus elements that effect long-distance regulation of class switch recombination. Immunity. 2001;15(2):187-199.

44. Vincent-Fabert C, Fiancette R, Pinaud E, et al. Genomic deletion of the whole IgH 3' regulatory region (hs3a, hs1,2, hs3b, and hs4) dramatically affects class switch recombination and Ig secretion to all isotypes. Blood. 2010;116(11):1895-1898.

45. Le Noir S, Boyer F, Lecardeur S, et al. Functional anatomy of the immunoglobulin heavy chain 3' super-enhancer needs not only core enhancer elements but also their unique DNA context. Nucleic Acids Res. 2017;45(10):5829-5837.

46. Morvan CL, Pinaud E, Decourt C, Cuvillier A, Cogné M. The immunoglobulin heavy-chain locus hs3b and hs4 3' enhancers are dispensable for VDJ assembly and somatic hypermutation. Blood. 2003;102(4):1421-1427.

47. Varano G, Raffel S, Sormani M, et al. The B-cell receptor controls fitness of MYC-driven lymphoma cells via GSK3β inhibition. Nature. 2017;546(7657):302-306.

48. Loddenkemper C, Anagnostopoulos I, Hummel M, et al. Differential Emu enhancer activity and expression of BOB.1/OBF.1, Oct2, PU.1, and immunoglobulin in reactive B-cell populations, B-cell non-Hodgkin lymphomas, and Hodgkin lymphomas. J Pathol. 2004;202(1):60-69.

49. McCune RC, Syrbu SI, Vasef MA. Expression profiling of transcription factors Pax-5, Oct-1, Oct-2, BOB.1, and PU.1 in Hodgkin's and non-Hodgkin's lymphomas: a comparative study using high throughput tissue microarrays. Mod Pathol. 2006;19(7):1010-1018.

50. Sartorelli V, Lauberth SM. Enhancer RNAs are an important regulatory layer of the epigenome. Nat Struct Mol Biol. 2020;27(6):521-528.

51. Arnold PR, Wells AD, Li XC. Diversity and Emerging Roles of Enhancer RNA in Regulation of Gene Expression and Cell Fate. Front Cell Dev Biol. 2020;7:377.

52. Pefanis E, Wang J, Rothschild G, et al. RNA exosome-regulated long non-coding RNA transcription controls super-enhancer activity. Cell. 2015;161(4):774-789.

53. Xiao S, Huang Q, Ren H, Yang M. The mechanism and function of super enhancer RNA. Genesis. 2021;59(5-6):e23422.

54. Dolloff NG. Discovery platform for inhibitors of IgH gene enhancer activity. Cancer Biol Ther. 2019;20(4):571-581.

Figure legends

Figure 1. Design and generation of a tiling CRISPRi library targeting IGH enhancers. A. Scheme of the human immunoglobulin heavy chain (*IGH*) locus. Green - *IGH* enhancers: two 3' regulatory regions (3'RR), which are composed of smaller enhancers (HS) and the intronic enhancer Eμ, composed of the core and two matrix attachment regions (MAR); black - immunoglobulin genes: C- constant, J – joining, D – diverse, V – variable. **B.** Summary of the sgRNA distribution in the CRISPR-eIGH library. Note that since 3'RR1 and 3'RR2 are highly similar, 2344 sgRNAs are common for both regions. **C.** SgRNA abundance in the CRISPR-eIGH library obtained with NGS. Red dotted lines indicate the 10^{th} (left) and 90^{th} (right) percentile. **D.** Overview of the CRISPRi screen experiment.

Figure 2. Tiling CRISPRi screen of the *IGH* enhancers in B-cell non-Hodgkin lymphoma cells. A. CRISPRi screen results. Scatterplots represent change of sgRNAs abundance relative to the initial pool in two screen replicates for each cell line. Numbers in the bottom left corner indicate the total number of sgRNA in the given cell line that were consistently >2-fold depleted from the initial pool. Black – sgRNAs targeting immunoglobulin heavy chain (*IGH*) enhancers, grey – non-targeting controls, red – positive controls targeting CD79. **B.** Fold change values of 20 consecutive sgRNA calculated using the sliding window approach. Colored boxes mark regions identified as essential for cell survival. For Eμ: chr14:106328838-106329184, pink box, 3'RR1 and 3'RR2: chr14:106152156-106153203 and chr14:106032312-106033352, blue box – peak 1, chr14:106162681-106163347 and chr14:106041116-106041795, green box – peak 2. C-**D.** GFP growth competition assay. Assay performed with individual sgRNAs over the course of 3 weeks in **C.** Burkitt lymphoma (BL) and **D.** diffuse large B-cell lymphoma (DLBCL) cell lines. Average and standard deviation from 3 independent biological replicates is shown. *, P ≤0.05, **, P≤0.01; ***, P≤0.001, mixed model analysis. **E.** Localization of breakpoints in the *IGH* locus for cell lines used in this study. Red – BL cell lines, purple – DLBCL cell lines.

Figure 3. **Transcriptional activity of *IGH* enhancers. A.** Chromatin-enriched RNA-Seq results for immunoglobulin heavy chain (*IGH*) enhancer regions accompanied by UCSC tracks from GM12878 B-cells: transcription and histone marks: H3K4me1 and H3K27ac – characteristic for enhancer regions and H3K4me3 – characteristic for promoters and active genes. Red – indicates reads from the plus strand, blue – indicates reads from the minus strand. Pink - Eμ peak, blue – 3'RRs peak 1, green – 3'RRs peak 2. **B.** Cellular localization of eRNA transcripts determined by cellular fractionation. Average and standard deviation from two biological replicates are shown. **C-D.** Validation of eRNA expression **C.** in a panel of B-cell lymphoma cell lines and control B cells: Burkitt lymphoma (BL) n=9, diffuse large B-cell lymphoma

(DLBCL) n=12: activated B-cell subtype (ABC) n=5, germinal center B-cell subtype (GCB) n=7, Hodgkin lymphoma (HL) n=8, control (germinal center B-cells) n=4. Expression normalized to TBP. ANOVA Kruskall-Wallis with Dunn's Multiple Comparison Post-Test was applied; *, P≤0.05; **, P≤0.01; ***, P≤0.001 **D.** in patient-derived FFPE samples: BL n=8 , DLBCL n=13: ABC n=7 , GCB n=6 , control (healthy donor tonsil) n=6. Expression normalized to TBP. ANOVA Kruskall-Wallis with Dunn's Multiple Comparison Post-Test was applied; *, P≤0.05; **, P≤0.01.

Figure 4. Downstream effects of targeting *IGH* enhancers. A. Expression of oncogenes involved in immunoglobulin heavy chain (*IGH*) translocation – MYC (DG75, BL41) or BCL2 (SUDHL4) and expression of eRNAs upon blocking of *IGH* enhancers essential regions on RNA level determined by qRT-PCR. Mean and standard deviation of three independent biological replicates are shown. Expression normalized to HPRT. *, P ≤ 0.05; **, P ≤ 0.01, ***, P ≤ 0.001, Mann-Whitney test. **B.** Immunostaining of B-cell receptor (BCR) on cell surface in DG75, BL41 (IgM) and SUDHL4 (IgG). Representative histograms of overlaid data for non-targeting controls (grey) and sgRNAs targeting *IGH*-enhancers essential regions (pink, Eμ peak; blue, 3'RR peak 1; green, 3'RR peak 2). Arrows indicate samples from a separate staining in SUDHL4. **C.** Average and SD of percentage of BCR-positive cells (surface IgM or IgG) from two biological replicates. *, P ≤ 0.05; **, P ≤ 0.01; ***, P ≤ 0.001; ****, P ≤ 0.001, Student's two-tailed t-test.

Figure 5. MYC overexpression rescues cell viability in BL cell line DG75 upon inhibition of *IGH* enhancer-essential regions. A. Overview of the MYC-rescue experiment. **B. and C.** Viability of **B.** DG75-MYC OE cell line and **C.** Control cell line DG75-EV transduced with sgRNAs targeting immunoglobulin heavy chain (*IGH*) enhancers and treated/untreated with doxycycline for induction of MYC expression. Average and standard deviation from three independent biological replicates are shown. *, P ≤ 0.05; **, P ≤ 0.01, Student's t-test.

A. Human, *IGH* locus, chr14

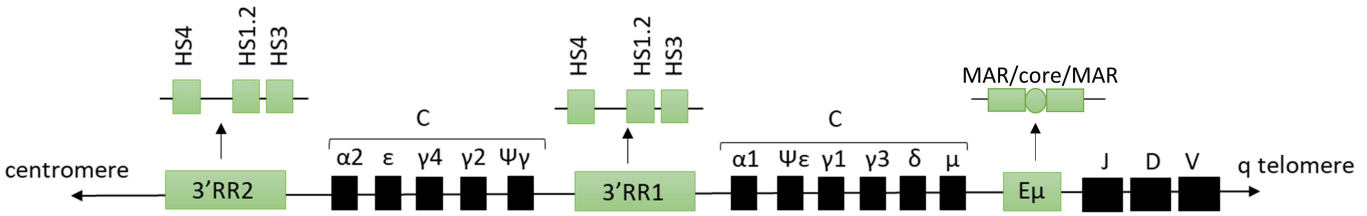

B.

Region	Localization (hg19)	Number of sgRNAs	Mean distance	Median distance	Min distance	Max distance
Eμ	chr14:106322800-106331124	2219	8.1	4	1	302
3'RR1	chr14:106145100-106176250	3784	10.7	4	1	1850
3'RR2	chr14:106024800-106050011	3322	10.6	4	1	1285

C.

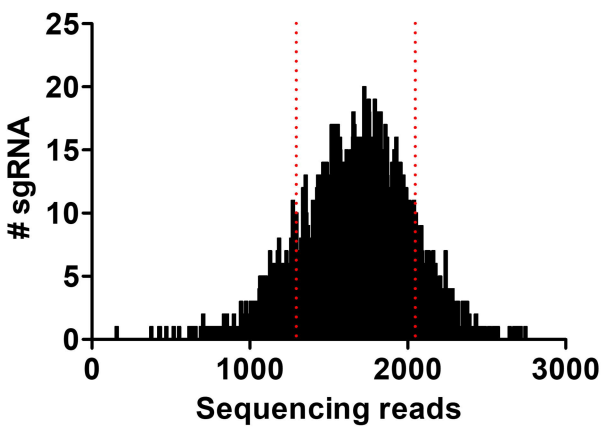

MiSeq analysis	
% sgRNAs with perfect match	88.6
% undetected sgRNAs	0.0
Skew ratio	1.58

D.

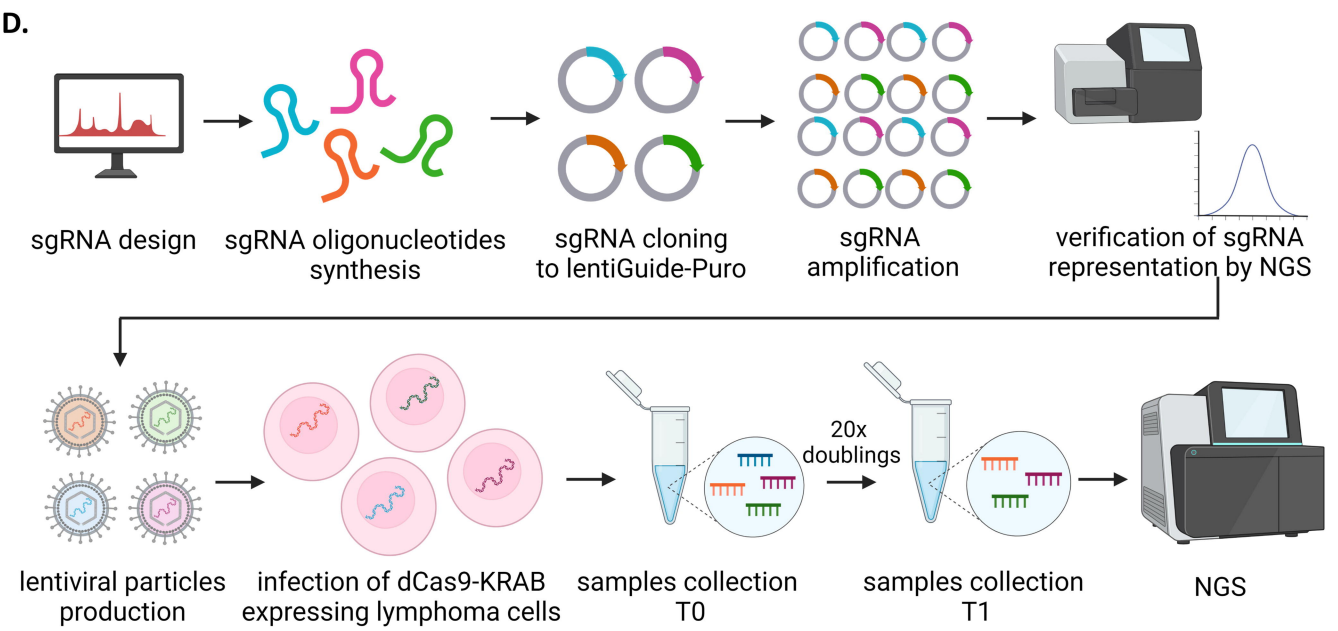

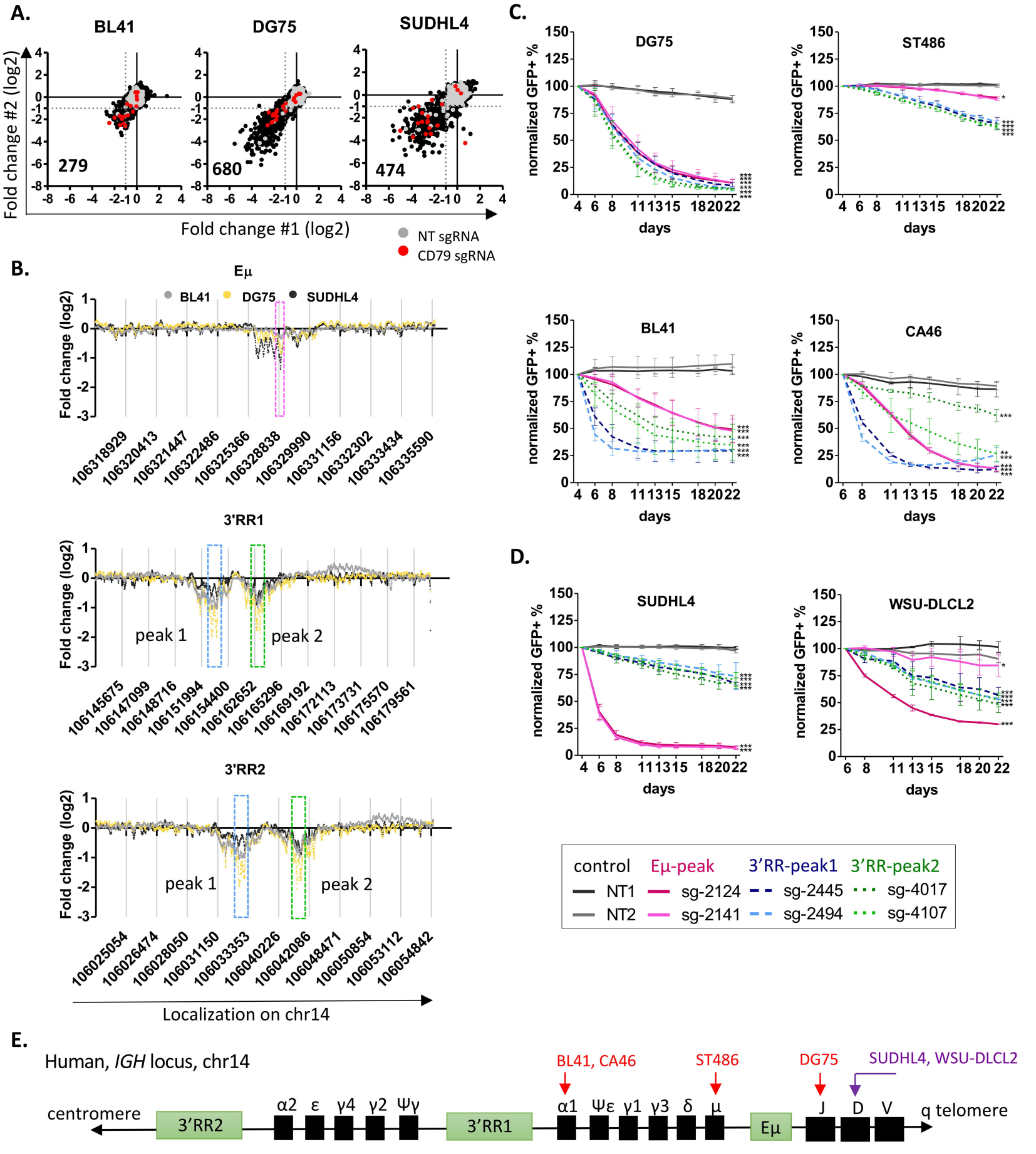
A.
BL41
DG75
SUDHL4
Fold change #2 (log2)
Fold change #1 (log2)
279
680
474
NT sgRNA
CD79 sgRNA
B.
Eμ
BL41 DG75 SUDHL4
Fold change (log2)
106318929 106320413 106321447 106322486 106325366 106328838 106329990 106331156 106332302 106333434 106335590
3'RR1
peak 1
peak 2
106145675 106147099 106148716 106151994 106154400 106162652 106165296 106169192 106172113 106173731 106175570 106179561
3'RR2
peak 1
peak 2
106025054 106026474 106028050 106031150 106033353 106040226 106042086 106048471 106050854 106053112 106054842
Localization on chr14
C.
DG75
ST486
BL41
CA46
normalized GFP+ %
days
D.
SUDHL4
WSU-DLCL2
control
Eμ-peak
3'RR-peak1
3'RR-peak2
NT1
NT2
sg-2124
sg-2141
sg-2445
sg-2494
sg-4017
sg-4107
E.
Human, IGH locus, chr14
BL41, CA46
ST486
DG75
SUDHL4, WSU-DLCL2
centromere
3'RR2
α2 ε γ4 γ2 Ψγ
3'RR1
α1 Ψε γ1 γ3 δ μ
Eμ
J D V
q telomere

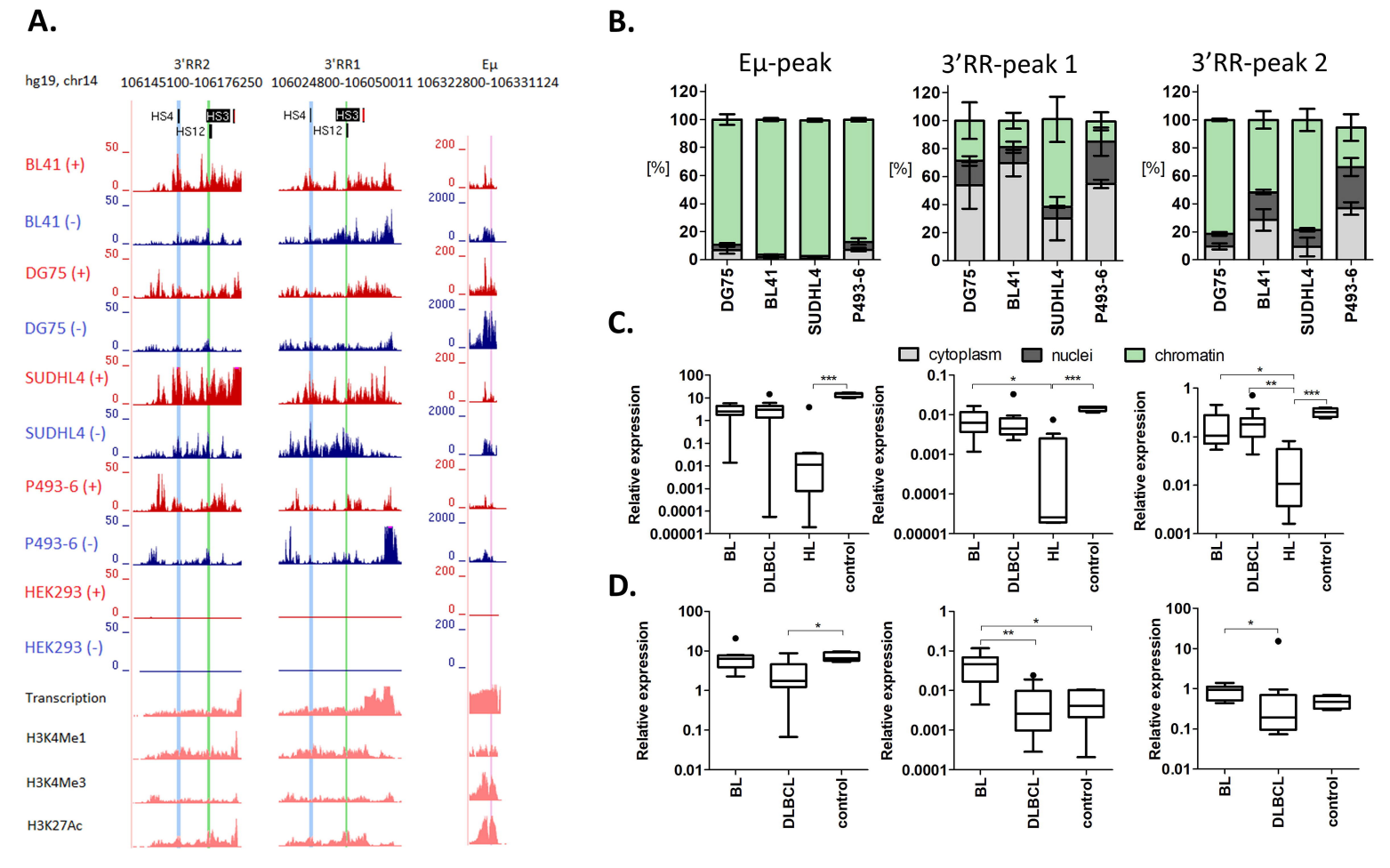
A.
hg19, chr14
3'RR2
106145100-106176250
3'RR1
106024800-106050011
Eμ
106322800-106331124
HS4
HS3
HS12
BL41 (+)
BL41 (-)
DG75 (+)
DG75 (-)
SUDHL4 (+)
SUDHL4 (-)
P493-6 (+)
P493-6 (-)
HEK293 (+)
HEK293 (-)
Transcription
H3K4Me1
H3K4Me3
H3K27Ac
B.
Eμ-peak
3'RR-peak 1
3'RR-peak 2
[%]
DG75
BL41
SUDHL4
P493-6
C.
cytoplasm
nuclei
chromatin
Relative expression
BL
DLBCL
HL
control
D.
Relative expression
BL
DLBCL
control

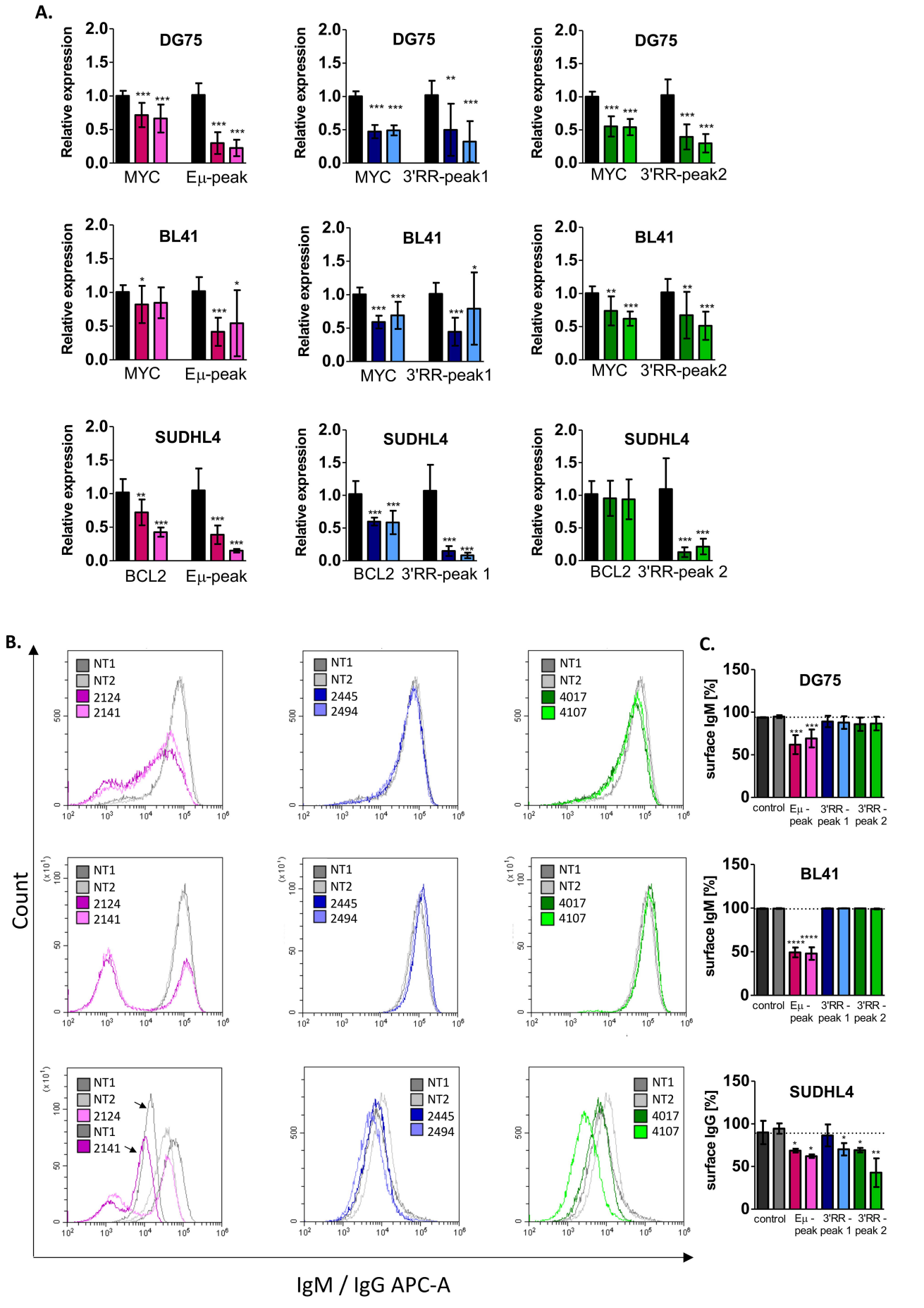
A.
DG75
BL41
SUDHL4
Relative expression
MYC
Eμ-peak
3'RR-peak1
3'RR-peak2
BCL2
B.
Count
IgM / IgG APC-A
NT1
NT2
2124
2141
2445
2494
4017
4107
C.
surface IgM [%]
surface IgG [%]
control
Eμ - peak
3'RR - peak 1
3'RR - peak 2

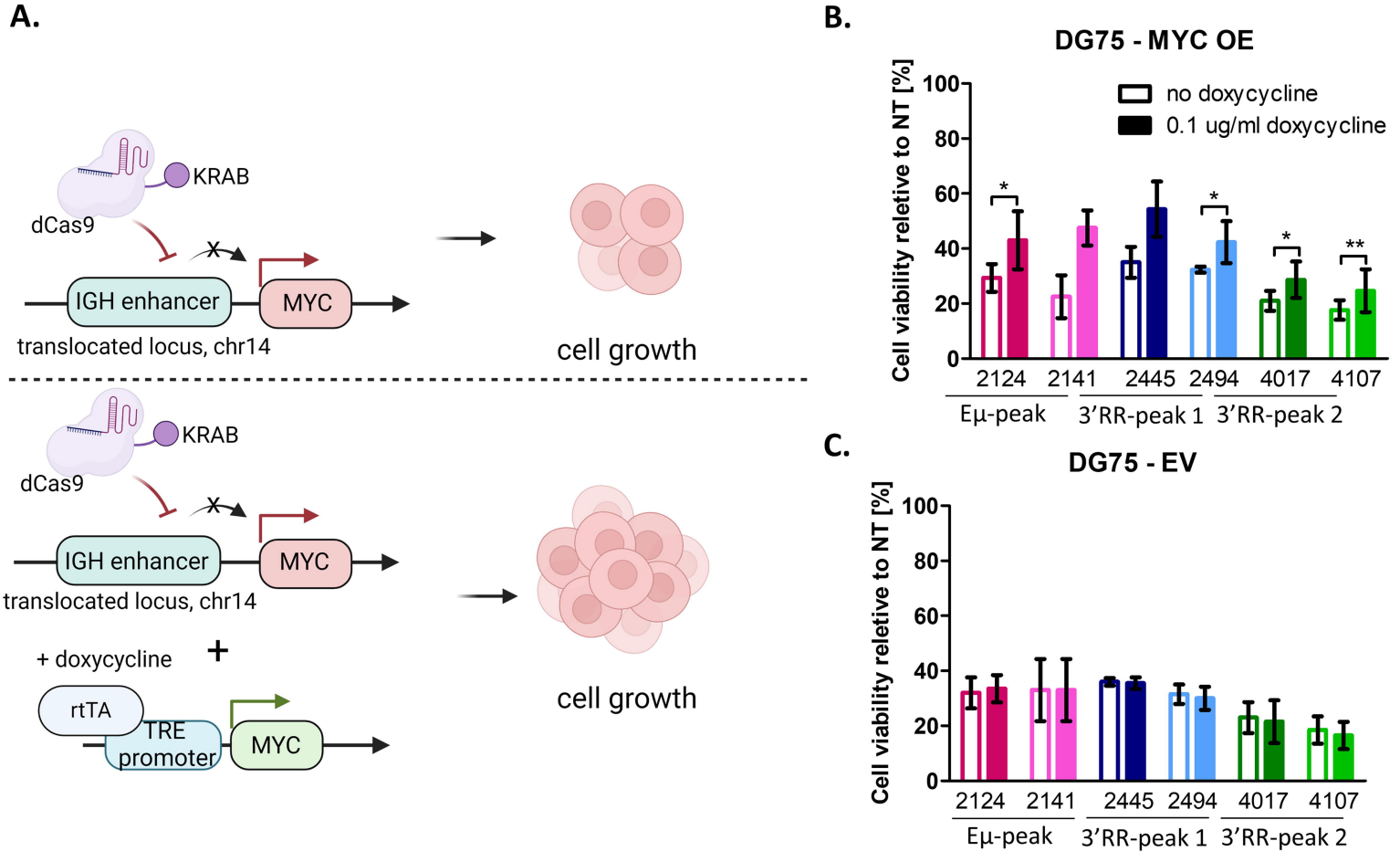
A.
KRAB
dCas9
IGH enhancer
MYC
translocated locus, chr14
cell growth
KRAB
dCas9
IGH enhancer
MYC
translocated locus, chr14
+ doxycycline
+
rtTA
TRE promoter
MYC
cell growth
B.
DG75 - MYC OE
no doxycycline
0.1 ug/ml doxycycline
Cell viability reletive to NT [%]
100
80
60
40
20
0
2124
2141
2445
2494
4017
4107
Eμ-peak
3'RR-peak 1
3'RR-peak 2
C.
DG75 - EV
Cell viability reletive to NT [%]
100
80
60
40
20
0
2124
2141
2445
2494
4017
4107
Eμ-peak
3'RR-peak 1
3'RR-peak 2

Core regions in immunoglobulin heavy chain enhancers essential for survival of non-Hodgkin lymphoma cells identified by a CRISPR interference screen

Marta Elżbieta Kasprzyk, Weronika Sura, Marta Podralska, Marta Kazimierska, Annika Seitz, Wojciech Łosiewski, Tomasz Woźniak, Jeroen E. J. Guikema, Arjan Diepstra, Joost Kluiver, Anke van den Berg, Natalia Rozwadowska, Agnieszka Dzikiewicz-Krawczyk

Supplementary Methods

Plasmids

Lenti-dCas9-KRAB-blast[1] (#89567) and lentiGuide-Puro[2] (#52963) were purchased from Addgene (Watertown, MA, USA) and used to establish NHL cell lines with stable expression of catalytically inactive Cas9 fused with KRAB domain and cloning of CRISPR-eIGH library, respectively. LentiGuide-Puro was also used for further validation of individual sgRNAs. pAW12.lentiguide.GFP[3] (#104374) purchased from Addgene was used in the GFP growth competition assays.

For MYC over-expression experiments (OE), the MYC ORF was cloned in the pCW57-MCS1-P2A-MCS2 (GFP) vector[4] (#80924, Addgene). This construct was used to establish DG75-dCas9-KRAB-MYC OE cell line with inducible MYC expression. Cells transduced with empty vector were used as controls.

For the production of lentiviral particles 2nd generation plasmids were used: envelope expressing plasmid pMD2.G (#12259, Addgene) and packaging plasmid psPAX2 (#12260, Addgene).

Design and generation of the CRISPR-eIGH library

In this study we aimed to target the *IGH* enhancer regions as defined by the H3K27ac histone mark plus 5 kb flanking sequences: Eμ (hg19 chr14:106317800-106336124), 3'RR1 (hg19 chr14:106140100-106181250) and 3'RR2 (hg19 chr14:106019800-106055011). The sequences were searched for the presence of the PAM sequence (5'-NGG-3') on both strands and all possible sgRNAs were listed using a custom Python script. Since 3'RR1 and 3'RR2 are highly homologous, numerous sgRNAs could target both regions, and those were allowed. Off-target binding of sgRNAs was checked using the Cas-OT script[5]. Only sgRNAs with at least three mismatches to the potential off-targets or at least two mismatches including at least one in the seed region (nt 9-20) were retained. We also included in the library 900 non-targeting sgRNAs from the Brunello library as a negative control[6] and 10 sgRNAs targeting regions -50 bp to +100 bp relative to TSS of CD79a and CD79b as positive controls. The list of all sgRNA oligonucleotides is provided in Supplementary Table 1.

Cloning of the CRISPR-eIGH library

Designed sgRNAs were ordered from Twist Bioscience (San Francisco, CA, USA) as oligonucleotides with the 20 nt sgRNA sequences flanked by sequences complementary to the lentiGuide-Puro vector TTTCTTGGCTTTATATATCTTGTGGAAAGGACGAAACACCG[sgRNA]GTTTTAGAGCTAGAAATAGCAAGTTAAAA TAAGGCTAGTCCGT. 2 ng of CRISPR-eIGH library was amplified with oligo-F and oligo-R primers (Supplementary Table 4) using NEBNext HiFidelity 2X PCR Master Mix (New England Biolabs, Ipswich,

MA, USA) in 20 x 25 µl PCR reactions. PCR program: 98°C 30 sec; (98°C 10 sec; 63°C 10 sec; 72°C 15 sec) x 6 cycles; 72°C 2 min. Pooled PCR reactions were purified using QIAquick PCR Purification Kit (Qiagen, Hilden, Germany). Purified PCR product was then run on agarose gel and extracted with QIAquick Gel Extraction Kit (Qiagen). LentiGuide-Puro was digested with BsmBI (New England Biolabs) and purified from agarose gel, same as oligo library. Purified sgRNA CRISPR-eIGH library was cloned into the lentiGuide-Puro vector using the circular polymerase extension cloning (CPEC) method as described previously[7]. Briefly, 20 CPEC reactions were performed with 10:1 insert:vector molar ratio (17 ng amplified oligos, 100 ng vector) and NEB Next HiFidelity 2X PCR Master Mix. PCR program: 98°C 30 sec; (98°C 10 sec; 72°C 4,5 min) x 5 cycles; 72°C 5 min. All PCR reactions were pooled and purified by isopropanol precipitation. 300 ng of the purified CPEC product was used for transformation of electrocompetent Endura cells (Lucigen, Middleton, WI, USA) according to the manufacturer's protocol. Three electroporations were performed giving in total ~7.7 million colonies and resulting in ~710x coverage of the library. Bacteria were spread on 245x245 mm agar plates and grown for 13 h at 37°C. Colonies were scraped off the plates and plasmid DNA was isolated using Plasmid Plus Maxi Kit (Qiagen). Quality of the cloned CRISPR-eIGH library was verified by MiSeq next generation sequencing on Illumina platform (Laboratory of High-Throughput Technologies, Adam Mickiewicz University, Poznań, Poland).

Cloning of individual sgRNA constructs

For cloning of individual sgRNAs into the lentiGuide-Puro and pAW12.lentiguide.GFP vectors, sense and antisense oligonucleotides containing overhangs compatible with BsmBI sticky ends (Supplementary Table 5) were synthesized by Genomed (Warsaw, Poland). They were resuspended in annealing buffer (10mM Tris-HCl pH 8, 1mM EDTA pH 8, 50mM NaCl) and annealed in a thermocycler under conditions: 95°C 5min, 95°C (-1°C/cycle) x 70 cycles. Annealed oligos were ligated into the BsmBI-digested lentiGuide-Puro and pAW12.lentiguide.GFP vectors at 1:5 vector:insert molar ratio with T4 DNA ligase (Invitrogen, Carlsbad, CA, USA). 1 µl of ligation reaction was used for transformation of JM109 competent cells (Promega, Madison, WI, USA). Plasmid DNA from single colonies was isolated using Plasmid Plus Maxi Kit (Qiagen) and the sequences were confirmed by Sanger sequencing (Genomed).

Generation of lentiviral particles

HEK293T cells were seeded in 6-well plates one day prior to transfection. Next day, ~80% confluent cells were transfected with 2nd generation packaging plasmids psPAX (1.5 µg) and pMD2.G (1 µg), together with 2 µg of the transfer plasmid using Lipofectamine 2000 (Invitrogen) or calcium phosphate method (Invitrogen). One day after transfection medium was replaced with fresh DMEM supplemented with 10% FBS. 48 h and 72 h post-transfection lentiviral supernatants were filtered through 0.45 µm filter and stored at -80°C.

Establishing cell lines with stable expression of dCas9-KRAB

1-2 x 10^6 of optimally dividing cells were transduced with 2nd generation lentiviral particles carrying lenti-dCas9-KRAB-blast. Briefly, cells were seeded on a 12-well plate, cell line-optimized virus amount was added along with 4 µg/ml polybrene and placed in 37°C incubator. For some cell lines spinfection was performed at 33°C, 1000 x g, 2h. After 24 h, transduced cell lines were washed in PBS and seeded for blasticidin (bln; Gibco, Grand Island, NY, USA) selection as indicated in Supplementary Methods Table 1. Antibiotic selection lasted 6 days. Genomic insertion of dCas9-KRAB expressing cassette was

confirmed on DNA level, followed by expression validation on RNA level by qRT-PCR and on protein level by Western Blot.

Supplementary Methods Table 1. Seeding densities and antibiotic concentrations used for cells selection after lentiviral transduction.

Cell line	Seeding density x10^6/ml	Puromycin concentration µg/ml	Blasticidin concentration µg/ml
BL41	0.25	1	2.5
CA46	0.15	2.3	5
DG75	0.17	3	20
ST486	0.25	0.3	8
LY91	0.3	1	5
JI	0.25	0.5	5
BL2	0.15	0.5	10
BL60	0.2	0.3	15
SUDHL4	0.3	1	10
WSU-DLCL2	0.3	1	15
P493-6	0.25	1	20
HEK293T	0.2	NA	5

NA - not applicable

Determination of virus titer and cell transduction with CRISPR-eIGH library

For CRISPRi screening experiment, the lentivirus titer was determined in order to transduce ca. 30% cells, which guarantees that approximately 85% of them are infected by a single construct[8]. For this purpose, 2.5 x 10^6 cells per well were plated in 12-well plate and transduced with various amounts of lentivirus in the presence of 4 µg/ml polybrene. After spinfection at 33°C, 1000 x g, for 2h 1 ml of medium was added. 24 h after transduction cells were washed and plated in duplicate with and without puromycin. Medium was changed after three days. After four days of selection cells were counted and the percentage of cells surviving puromycin treatment relative to cells without puromycin was calculated. Based on this, the amount of virus resulting in ~30% surviving cells was determined.

For the CRISPR screen, 27.5 x 10^6 cells were transduced in duplicate with CRISPR-eIGH library, with the previously established amount of virus. After four days of selection with puromycin (T0) 8 x 10^6 cells were collected for DNA isolation. Remaining cells were further cultured for 20 population doublings. At each passage, the number of cells corresponding to 1,000x coverage of the library, that is 8 x 10^6, were cultured in RPMI medium with 1 µg/ml (DG75) or 0.3 µg/ml (other cell lines) puromycin and collected at the final timepoint (T1).

Preparation of libraries for next-generation sequencing of the plasmid pool or genomic DNA

sgRNA sequences from the CRISPR-eIGH library plasmids were amplified as described previously[9]. Briefly, PCR reactions were performed using High-Fidelity MasterMix 2x (New England Biolabs, #M0541L) and primers incorporating Illumina adaptors (Supplementary Table 6). PCR products were purified with QIAquick PCR Purification Kit (Qiagen, #28106), then analyzed by DNA electrophoresis and extracted from agarose gel with QIAquick Gel Extraction Kit (Qiagen, #28706). Prior to NGS, the

quality and quantity of library were determined using KAPA Library Quantification Kit (Roche, #07960140001).

To analyze the sgRNA representation in the screening experiments, genomic DNA from cell lines was isolated using GENTRA Puregene Kit (Qiagen, #158722) and then sgRNA sequences were amplified as described above. DNA from 8 x 10^6 cells was amplified in 30 (BL41, DG75) or 40 (SUDHL4) individual 50 µl PCR reactions per sample with 2-2.5 µg DNA input.

NGS and data analysis

NGS was performed on Illumina X-Ten platform at BGI (Hong-Kong). Adaptor sequences were removed, and reads were split for individual samples based on specific barcodes. Supplementary Table 2 summarizes the number of reads obtained for each sample. A Python script[10] was used for sgRNA enumeration. Only reads with no mismatches to sgRNA sequences were counted. Next, fold change (FC) between the beginning and end of screen was calculated for each sgRNA. FC values for both screen replicates were averaged. To identify regions whose targeting significantly affected lymphoma cell growth, we applied the sliding window approach[11]. Average FC values were calculated for 20 consecutive sgRNAs (Supplementary Table 3). Significance was calculated with t-test comparing FC values for 20 sgRNAs in each window with the negative control sgRNAs. We considered as significant windows which were at least 1.5-fold depleted (log2FC -0.585) and with FDR<0.001.

Cellular fractionation

20 x 10^6 cells (30 x 10^6 for SUDHL4) were used for cellular fractionation as described previously[12]. All steps were performed on ice. Buffers were supplemented with DTT (if noted), 1x EDTA-free protease inhibitors and 40U/ml RNaseOUT (Invitrogen) directly before use and kept on ice. Briefly, cells were washed in ice-cold PBS. Then cell pellet was resuspended in 500 µl Buffer W (300 mM sucrose, 10 mM Tris-HCl pH 8.0, 10 mM NaCl, 2 mM $MgAc_2$ 0.5 mM DTT), followed by addition of 500 µl Buffer L (Buffer W supplemented with 6 mM $CaCl_2$, 0.2 % IGEPAL CA-630, 0.5 mM DTT). Lysates were centrifuged 1000 x g, 4°C, 10 min. Resulting supernatant was saved as cytoplasmic fraction, while nuclear pellet was processed further. Nuclei were washed in Buffer G (50 mM Tris-HCL pH 8.0, 25% glycerol, 5 mM $MgAc_2$, 0.1 mM EDTA, 5 mM DTT), then lysed with Buffer U (1 M urea, 20 mM HEPER pH 7.5, 7.5 mM $MgCl_2$, 0,1 mM EGTA, 300 mM NaCl, 1 mM DTT), vortexed and centrifuged 20 000 x g, 4°C, 10 min. Resulting supernatant was saved as nuclear fraction, while chromatin pellet was washed twice in Chromatin Wash Buffer (50 mM Tris-HCl pH 8.0 supplemented with 40 U/ml RNaseOUT). Chromatin pellet was then sonicated twice [5 sec on, 30 sec off] (Misonix 3000; Misonix, Farmingdale, NY, USA) on ice in 300 µl Buffer G for RNA isolation or in 500 µl RIPA buffer (Sigma, Saint Louis, MO, USA) supplemented with protease inhibitors for protein extraction. RNA was isolated from each fraction using Trizol method. Additionally, 10 µl 500 mM EDTA was added to chromatin fraction and heated 10 min 65°C with 600 rpm shaking on thermoblock. RNA and protein samples were stored in -80°C until analysis. To confirm successful separation of the fractions on RNA level, 2 marker genes were used per each fraction: RPPH1 and DANCER for cytoplasm, U3SNO and MIAT for nuclei and TBP_intron and KTN1_AS1_intron for chromatin (primers listed in Supplementary Table 4). To additionally confirm that the fractionation was successful, Western Blot was performed with fraction-specific antibodies (Supplementary Table 7), as described in Supplementary Methods section **Western Blot**.

Chromatin-enriched RNA-Seq and data analysis

RNA from chromatin fraction of two biological replicates per each cell line was tested on 2% agarose gel for integrity. Prior to sequencing, RNA was treated with TURBO-DNase (Thermo Fisher Scientific, Waltham, MA, USA) according to manufacturer instructions, followed by purification using RNA Clean & Concentrator (Zymo Research, Irvine, CA, USA) with additional DNase treatment on the column. RNA-Seq stranded library preparation, pair-end sequencing and bioinformatic data analysis were performed by Novogene (Beijing, China). Ribo-zero rRNA Removal Kit (Epicentre, Paris, France) and NEBNext Ultra Directional RNA Library Prep Kit for Illumina (NEB) were used for library preparation. Sequencing was performed on Illumina X-Ten platform. Quality control of raw data in FASTQ format was performed, clean data were obtained by removing reads containing adapter and poly-N sequences and reads with low quality.. Approximately 77-92 x 10^6 clean reads were obtained per sample. All downstream analyses were based on clean data with high quality. Reads were mapped to the human reference genome version GRCh37.87 using HISAT 2 software. Reads mapping to the *IGH* enhancer regions (see **Design of the CRISPR-eIGH library**) were selected for further study. Using Galaxy[13] BAM files provided by Novogene were sliced by genomic region chr14:106019800-106337000 and filtered by second mate to retrieve information about the strand from which the transcript was derived. Next, using Integrative Genome Browser[14], BedGraph files were generated and visualized in UCSC Genome Browser (http://genome.ucsc.edu)[15].

RNA isolation, cDNA synthesis and RT-qPCR

RNA was isolated from 1-2 x 10^6 cells using RNA MiniPrep (Zymo Research, Irvine, CA, USA) according to the manufacturer's instructions. DNase treatment was performed on the column. To obtain RNA from cellular fractions Trizol method was applied. Briefly, samples were resuspended in TRI Reagent (Sigma), chromatin fraction was additionally heated as described in Supplementary Methods section **Cellular fractionation.** Samples were then mixed with chloroform and centrifuged according to manufacturer's instructions. Next, RNA was precipitated with 96-99.9 % ethanol, 300 mM NaCl and 15 µg GlycoBlue Coprecipitant (Invitrogen) at -20^{o}C over-night. Next day, the RNA pellet was washed in 75% ethanol and resuspended in UltraPure RNAse-free water. Chromatin fraction was additionally treated with TURBO-DNase (Invitrogen) according to the manufacturer's instructions. Next, RNA from all fractions was purified and DNase treated on the column using RNA Clean and Concentrator (ZYMO Research). Reverse transcription was performed using 300-1,000 ng of total RNA or RNA fractions with QuantiTect Reverse transcription Kit (Qiagen) or SuperScript III and random primers (both Thermo Fisher Scientific).

qPCR analysis was performed using 5-15 ng cDNA with PowerUp SYBR Green Master Mix (Thermo Fisher Scientific) on CFX96 Touch qPCR System (Bio-Rad, Hercules, CA, USA). Gene expression was normalized relative to the housekeeping gene. For eRNA expression validation in larger panel of B-cell cell lines and in FFPE patient samples qPCR was done with 2X SYBR Green Master Mix (Applied Biosystems B.V., Bleiswijk, The Netherlands) on Light Cycler 480 (F. Hoffmann-La Roche, Basel, Switzerland). All primer sequences used in this study are available in Supplementary Table 4.

Validation of enhancer RNA expression

To validate eRNA expression and cellular localization, primers specific for transcriptionally active core *IGH* regions, based on chromatin-enriched RNA-seq, were designed. Primers detected transcripts from

both the plus and minus strands. eRNA expression was verified in a panel of B-cell lines and in patient-derived samples (described in Supplementary Methods section **Patient samples**). Cell panel consisted of 9 BL cell lines: EBV-negative - DG75, CA46, ST486, BL41, Ramos and EBV-positive - BL65, Namalwa, Jijoye, Raji; 12 DLBCL: GCB type - SUDHL16, SUDHL10, SUDHL6, SUDHL5, SUDHL4, SC1, WSU-DLCL2 and ABC type - U2932, Ocily3, RI-1, Nu-dul1, SUDHL2; 8 Hodgkin lymphoma (HL) cell lines: L428, L1236, KMH2, DEV, L540, L591, SUPHD1, HDLM2 and 4 germinal center B-cell samples as controls[16].

GFP competition assay

0.5-1 x 10^6 cells were transduced with individual sgRNA constructs in pAW12.lentiguide.GFP and cultured for 22 days. Cells were analyzed three times a week by flow cytometry using CytoFLEX S (Beckman Coulter, Indianapolis, IN, USA). The percentage of GFP-positive cells was calculated in reference to the start of the experiment (day 4 or day 6) set as 100%.

B-cell receptor (BCR) immunostaining

1 x 10^6 cells per sample were collected and washed with PBS, then with ice-cold staining buffer (2% FBS in PBS). Cells were resuspended in 95 µl of ice-cold staining buffer with addition of 5 µl FcR blocking reagent, human, (MiltenyiBiotec, Bergisch Gladbach, Germany, #130-059-901) and incubated 10 min in a fridge. Then, 20 µl of APC Mouse Anti-Human IgM (BD Biosciences, Franklin Lakes, NJ, USA, #551062) or 0.1 µg of Goat F(ab')2 Anti-Human IgG-AF647 (Southern Biotech, Birmingham, AL, USA, 2042-31) was added and cells were incubated 25 min on ice, protected from light. Next, cells were washed twice with 2 ml of staining buffer and finally resuspended in 100 µl of this buffer for flow cytometry analysis, performed on CytoFLEX S (Beckman Coulter).

MYC overexpression

1 x 10^6 DG75-dCas9-KRAB cells were transduced with 2nd generation lentiviral particles carrying pCW57-MCS1-P2A-MCS2-MYC OE (GFP) or empty vector (EV). GFP-positive cells were sorted in PBS supplemented with 1% FBS and collected in culture medium supplemented with 50% FBS in 5 ml cytometric tubes. DG75-dCas9-KRAB-MYC OE cells were sorted on SH800S cell sorter (Sony Biotechnology, San Jose, CA, USA) using 100 µM nozzle, normal mode. DG75-dCas9-KRAB-EV cells sorting was carried out using the BD FACS AriaIII (Becton Dickinson, Franklin Lakes, NJ, USA) cell sorter using 100 µM nozzle, 20 psi (0,138 MPa), 4-way sorting purity mode was selected for gaining highest purity level. After sorting cells were seeded at high density 1 x 10^6 cells/ml in complete RPMI medium and then split depending on cell fitness. MYC overexpression upon addition of doxycycline (Merck, Darmstadt, Germany) was evaluated on RNA and protein level. To assess cell survival upon MYC overexpression, DG75-MYC-OE cells were mixed 1:1 with DG75-dCas9 (no GFP, no ectopic MYC overexpression) and GFP growth competition assay was performed for 3 weeks. For the rescue experiment, 1 x 10^6 DG75-dCas9-KRAB-MYC OE and EV cells were transduced with 2nd generation lentiviral particles carrying individual sgRNAs cloned into lentiGuidePuro, followed by puromycin selection.

Cell viability assay

Cell viability was measured using CellTiter-Glo Luminescent Cell Viability Assay (Promega, Madison, WI, USA). Briefly, at day 6 post-infection, 2000 cells per well were seeded on 96-well plates in triplicate. Doxycycline was added to the final concentration of 0.1 µg/ml. As control, wells without doxycycline

were prepared. CellTiter-Glo reagent was mixed 1:2 in PBS and 100 µl per well was added. Luminescence was measured on GloMax-Multi Detection System (Promega) at 1h (baseline) and 72h after seeding cells. Cell viability was determined as the relative luminescence (RLU) calculated relative to the first measurement (1h). For each experiment three biological replicates were made. Change in cell growth upon doxycycline administration in cells infected with sgRNAs targeting *IGH* enhancers was calculated relative to the non-targeting controls.

Western Blot

5-20 x 10^6 cells were washed in PBS, then lysed in RIPA buffer (Sigma, Saint Louis, MO, USA), supplemented with protease inhibitors. Protein concentration was determined using Bicinchoninic Acid Kit (Sigma). 20 µg of total protein was mixed with the Laemmli 4X sample buffer (Sigma), heat-denatured and separated at 120V on the 8% (for Cas9 detection) or 12% polyacrylamide gel (PAA, acrylamide:bisacrylamide, 49:1) supplemented with 2,2,2-trichloroetanol (Merck, Kenilworth, NJ, USA) to allow for stain-free total protein detection. For cellular fractionation control, an equal portion of each faction was loaded on 12 % PAA. Proteins were transferred onto PVDF (Bio-Rad, #1620177) or Low Fluorescence PVDF (Bio-Rad, #1620264) membrane for 1.5h 75V at room temperature with cooling, blocked for 1h in 5% milk in TBST and incubated with primary antibody at 4°C overnight. Next membranes were washed in TBST, followed by TBS wash and incubated with secondary HRP-conjugated antibody for 1h at room temperature. Signal was detected by chemiluminescence using Clarity Western ECL Substrate (Bio-Rad) with ChemiDoc Imaging Systems (Bio-Rad). Quantitative analysis was performed using Image Lab Software (Bio-Rad). For expression analysis bands were normalized using total protein method. Full list of antibodies used in this study can be found in Supplementary Table 7.

Statistical analysis

In eRNA expression validation, difference in expression between tested groups was evaluated with ANOVA Kruskall-Wallis with Dunn's Multiple Comparison Post-Test. For the other qRT-PCR results the Mann-Whitney test was applied. BCR staining was analyzed with Student's two-tailed t-test and cell viability change upon MYC overexpression with Student's paired one-tailed t-test. Those statistical analyses were calculated with GraphPad Prism version 5.0.0 (GraphPad Software Inc., San Diego, CA, USA) with a P-value significance cut-off $P<0.05$. Statistics for GFP-growth competition assay was calculated as described previously[17] using SPSS software (IBM, Armonk, NY, USA). Mixed model analysis was used for comparison of GFP-positive cells decrease over time between controls and samples with blocked *IGH*-enhancers essential regions, time and the interaction of time and given sgRNA were treated as fixed effects and the measurement repeat for a given sgRNA as random effect.

References

1. Xie, S. *et al.* Multiplexed Engineering and Analysis of Combinatorial Enhancer Activity in Single Cells. *Mol. Cell* **66**, 285-299.e5 (2017).
2. Sanjana, N. E. *et al.* Improved vectors and genome-wide libraries for CRISPR screening. *Nat. Methods* **11**, 783–784 (2014).
3. Weintraub, A. S. *et al.* YY1 Is a Structural Regulator of Enhancer-Promoter Loops. *Cell* **171**, 1573-1588.e28 (2017).
4. Barger, C. J. *et al.* Pan-Cancer Analyses Reveal Genomic Features of FOXM1 Overexpression in Cancer. *Cancers (Basel).* **11**, (2019).
5. Xiao, A. *et al.* CasOT: a genome-wide Cas9/gRNA off-target searching tool. *Bioinformatics* **30**, 1180–1182 (2014).

6. Doench, J. G. *et al.* Optimized sgRNA design to maximize activity and minimize off-target effects of CRISPR-Cas9. *Nat. Biotechnol.* **34**, 184–191 (2016).
7. Quan, J. & Tian, J. Circular polymerase extension cloning of complex gene libraries and pathways. *PLoS One* **4**, (2009).
8. Doench, J. G. Am I ready for CRISPR? A user's guide to genetic screens. *Nat. Rev. Genet.* **19**, 67–80 (2018).
9. Kazimierska, M. *et al.* CRISPR/Cas9 screen for genome-wide interrogation of essential MYC-bound E-boxes in cancer cells. *Mol. Oncol.* (2023) doi:10.1002/1878-0261.13493.
10. Joung, J. *et al.* Genome-scale CRISPR-Cas9 knockout and transcriptional activation screening. *Nat. Protoc.* **12**, 828–863 (2017).
11. Fulco, C. P. *et al.* Systematic mapping of functional enhancer-promoter connections with CRISPR interference. *Science* **354**, 769–773 (2016).
12. Winkle, M. *et al.* The lncRNA KTN1-AS1 co-regulates a variety of Myc-target genes and enhances proliferation of Burkitt lymphoma cells. *Hum. Mol. Genet.* **31**, 4193–4206 (2022).
13. Afgan, E. *et al.* The Galaxy platform for accessible, reproducible and collaborative biomedical analyses: 2016 update. *Nucleic Acids Res.* **44**, W3–W10 (2016).
14. Freese, N. H. *et al.* Integrated genome browser: visual analytics platform for genomics. *Bioinformatics* **32**, 2089–2095 (2016).
15. Kent, W. J. *et al.* The Human Genome Browser at UCSC. *Genome Res.* **12**, 996–1006 (2002).
16. Ziel-Swier, L. J. Y. M. *et al.* The Role of the MYC/miR-150/MYB/ZDHHC11 Network in Hodgkin Lymphoma and Diffuse Large B-Cell Lymphoma. *Genes (Basel).* **13**, (2022).
17. Niu, F. *et al.* The mir-26b-5p/kpna2 axis is an important regulator of burkitt lymphoma cell growth. *Cancers (Basel).* (2020) doi:10.3390/cancers12061464.

Supplementary Materials

Supplementary Figures:

Supplementary Tables:

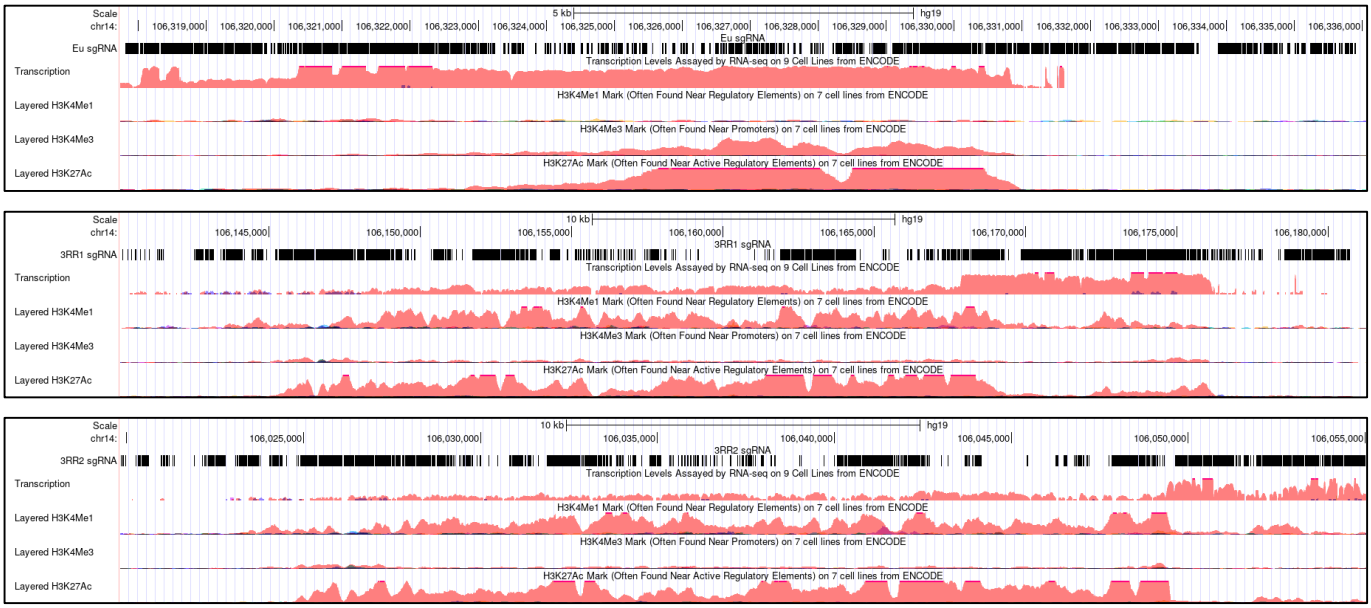

Supplementary Figure 1. IGH regions used for the design of the CRISPR-eIGH library. Black lines indicate localization of sgRNAs oligonucleotides. From the top: Eμ, 3'RR1 and 3'RR2. Peaks represent UCSC tracks : transcription, H3K4me1, H3K4me3, H3K27ac of GM12878 B-cells from ENCODE.

A.

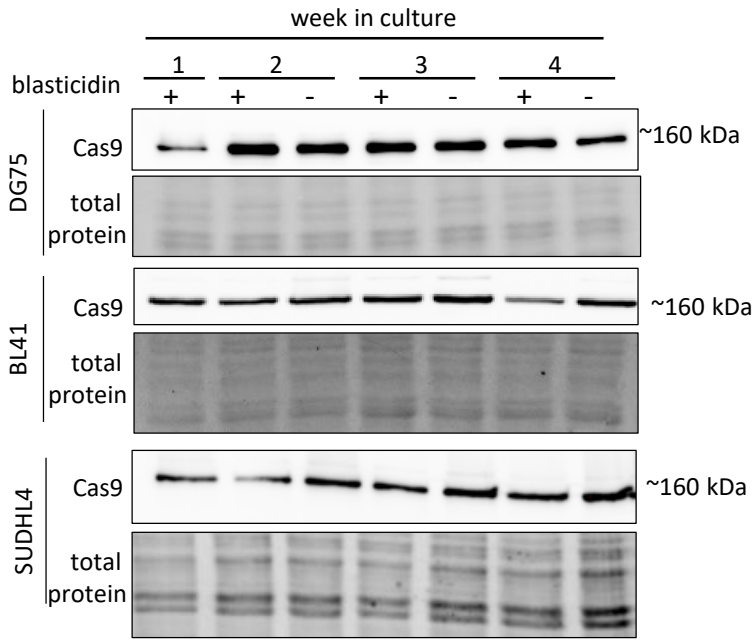

B.

Experiment	Percent of transduced cells	Number of transduced cells	CRISPR-eIGH library coverage
BL41 screen #1	25.1 %	6.9 M	860x
BL41 screen #2	28.1 %	7.7 M	965x
DG75 screen #1	30.4 %	8.4 M	1045x
DG75 screen #2	21.8 %	6 M	750x
SUDHL4 screen #1	28.4 %	7.8 M	975x
SUDHL4 screen #2	22.6 %	6.2 M	775x

Supplementary Figure 2. **A.** Verification of dCas9 expression on protein level over time with or without addition of blasticidin in cell lines used in CRISPRi screens. **B.** CRISPRi screens details for each replicate.

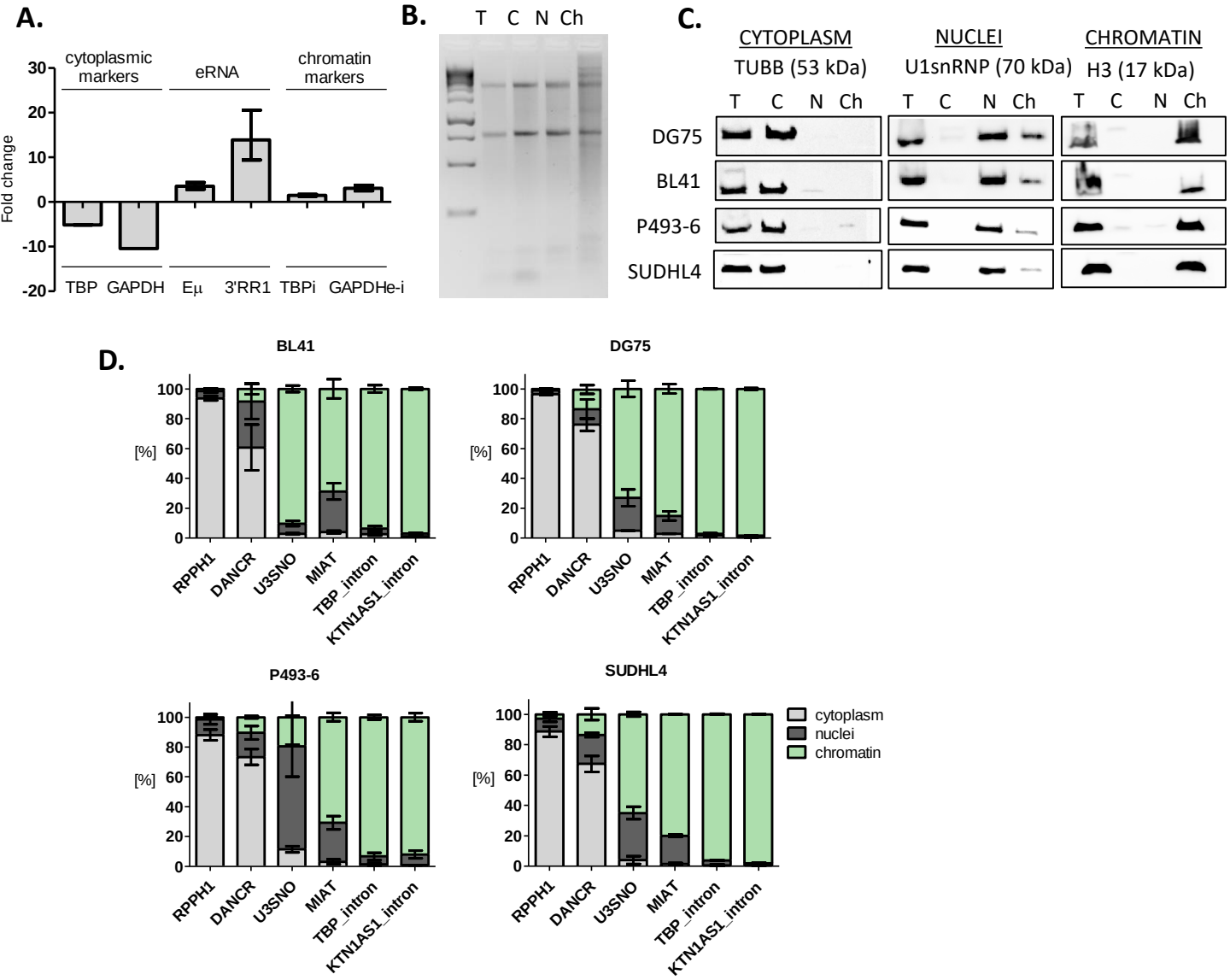

Supplementary Figure 3. **Subcellular RNA fractionation. A.** Abundance of transcripts in the chromatin fraction relative to total RNA. Cytoplasmic markers target spliced transcripts, while chromatin markers target unspliced transcripts. TBPi – intron, GAPDHe-i – transcript from exon-intron boundary. *IGH* enhancer RNA transcripts were predicted based on available transcription data from GM12878 cells (ENCODE). **B.** RNA from cellular fractionation on 2% agarose gel. Enrichment of small RNAs is visible in the cytoplasmic fraction. In chromatin fraction the pattern of observed ribosomal RNAs differs due to presence of rRNA precursors. T – total RNA, C – cytoplasmic fraction, N – nuclear fraction, Ch – chromatin fraction. **C.** Cellular fractionation control on protein level. T – total protein, C – cytoplasmic fraction, N – nuclear fraction, Ch – chromatin fraction. Fraction markers: cytoplasm – TUBB, nuclei – U1 snRNP 70, chromatin – H3. A representative blot is shown. **D.** Cellular fractionation control on RNA level. Fraction markers: cytoplasm – RPPH1, DANCR, nuclei – U3SNO, MIAT, chromatin – introns of TBP and KTN1_AS1. Average and SD from two independent biological replicates is shown.

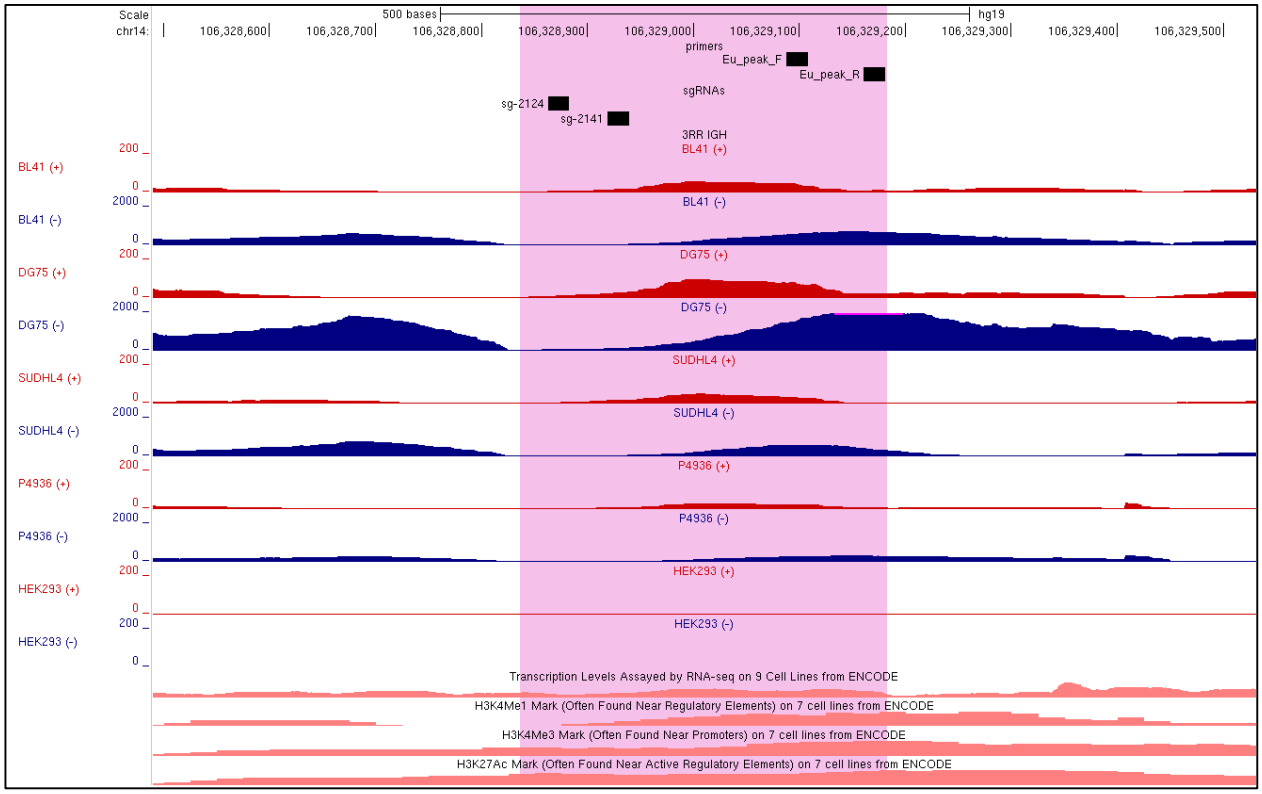

Supplementary Figure 4. UCSC Genome Browser zoom in on IGH Eμ enhancer. CRISPRi-identified enhancer-essential region is highlighted in pink. Localization of sgRNAs and primers used in CRISPRi screens and eRNA expression validation is marked as black boxes. Presented coverage are reads obtained from chromatin-enriched RNA-Seq. Red – reads from the plus strand, blue – reads from the minus strand obtained from chromatin-enriched RNA-Seq. Bottom tracks represent transcription and layered histone marks of GM12878 cells from ENCODE.

A.

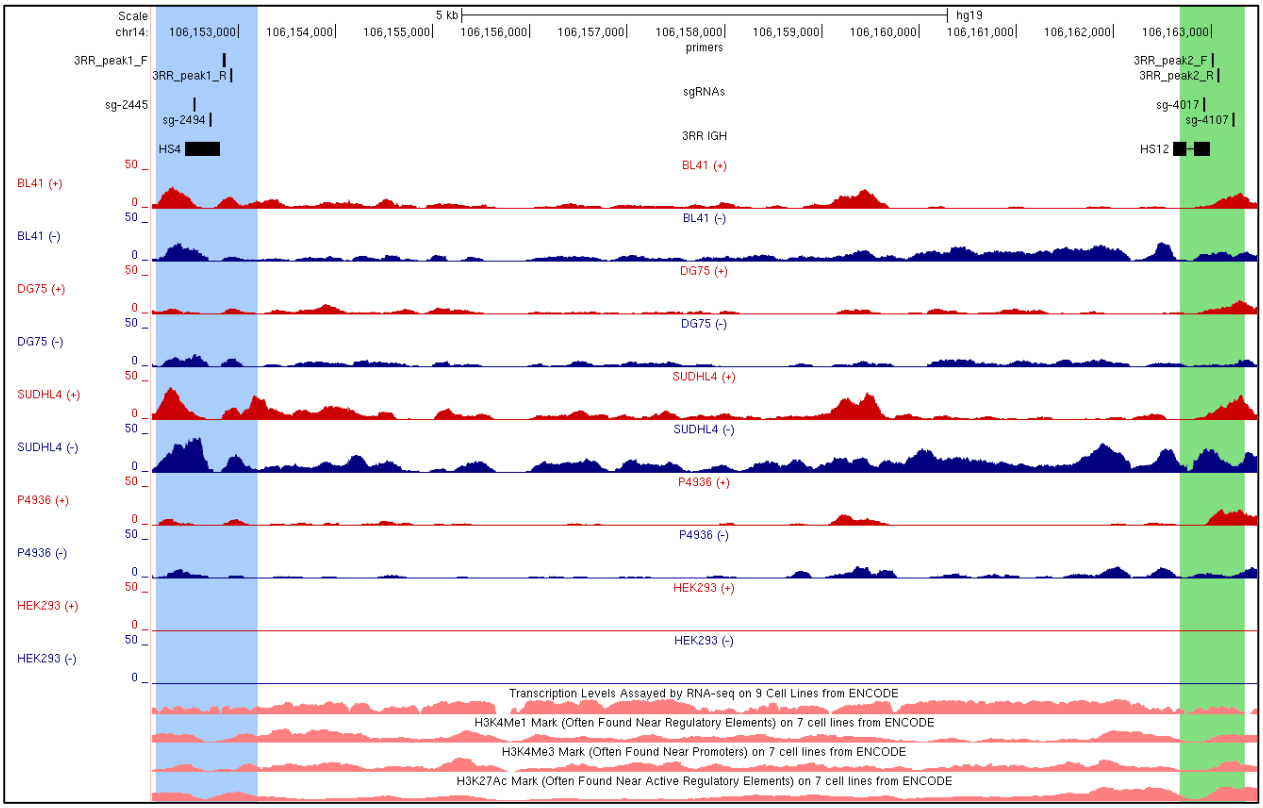

B.

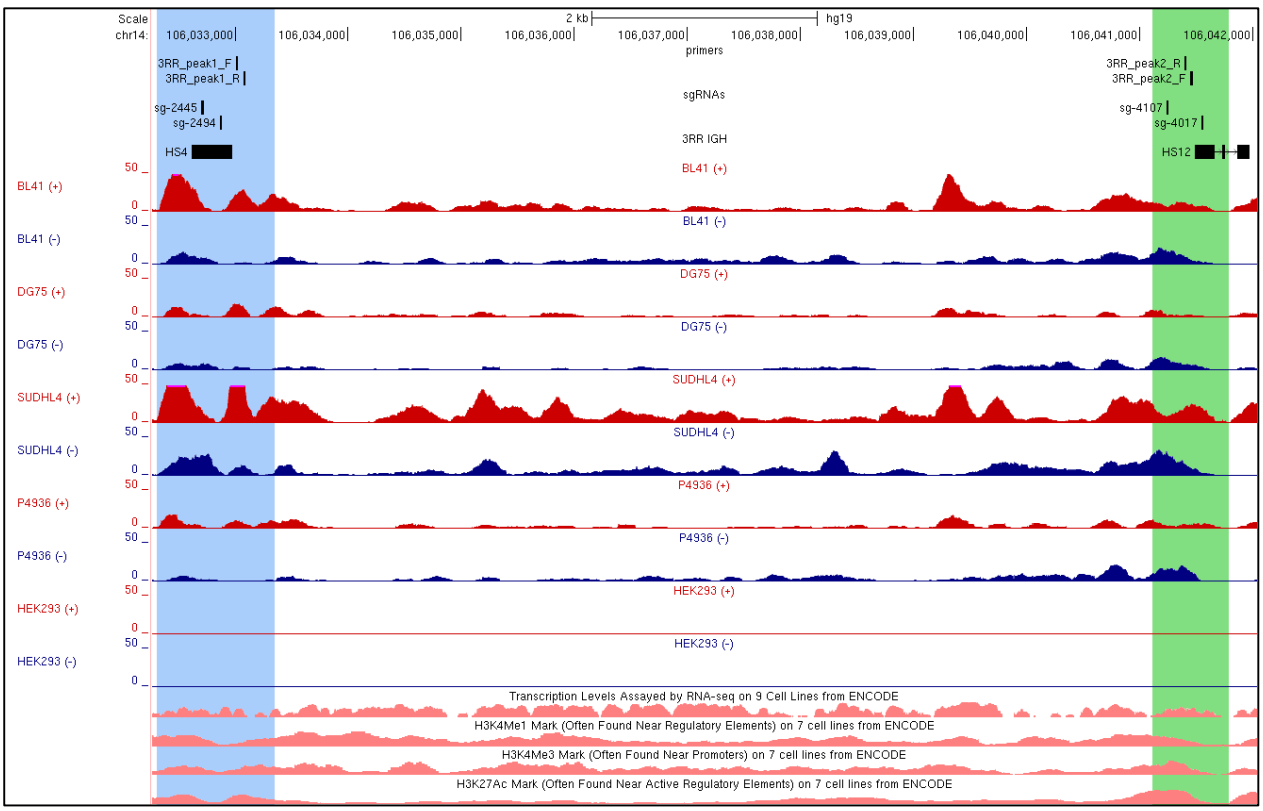

Supplementary Figure 5. **UCSC Genome Browser zoom in on *IGH* 3'RR enhancers regions.** Presented coverage are reads obtained from chromatin-enriched RNA-Seq. Red – reads from the plus strand, blue – reads from the minus strand obtained from chromatin-enriched RNA-Seq. Localization of primers and sgRNAs used in CRISPRi screens and eRNA expression validation is marked as black boxes. **A.** 3'RR1 enhancer and enhancer-essential region 1 (peak 1) highlighted in blue and region 2 (peak 2) in green. **B.** 3'RR2 enhancer and enhancer-essential region 1 (peak 1) highlighted in blue and region 2 (peak 2) in green. Bottom tracks represent transcription and layered histone marks of GM12878 cells from ENCODE

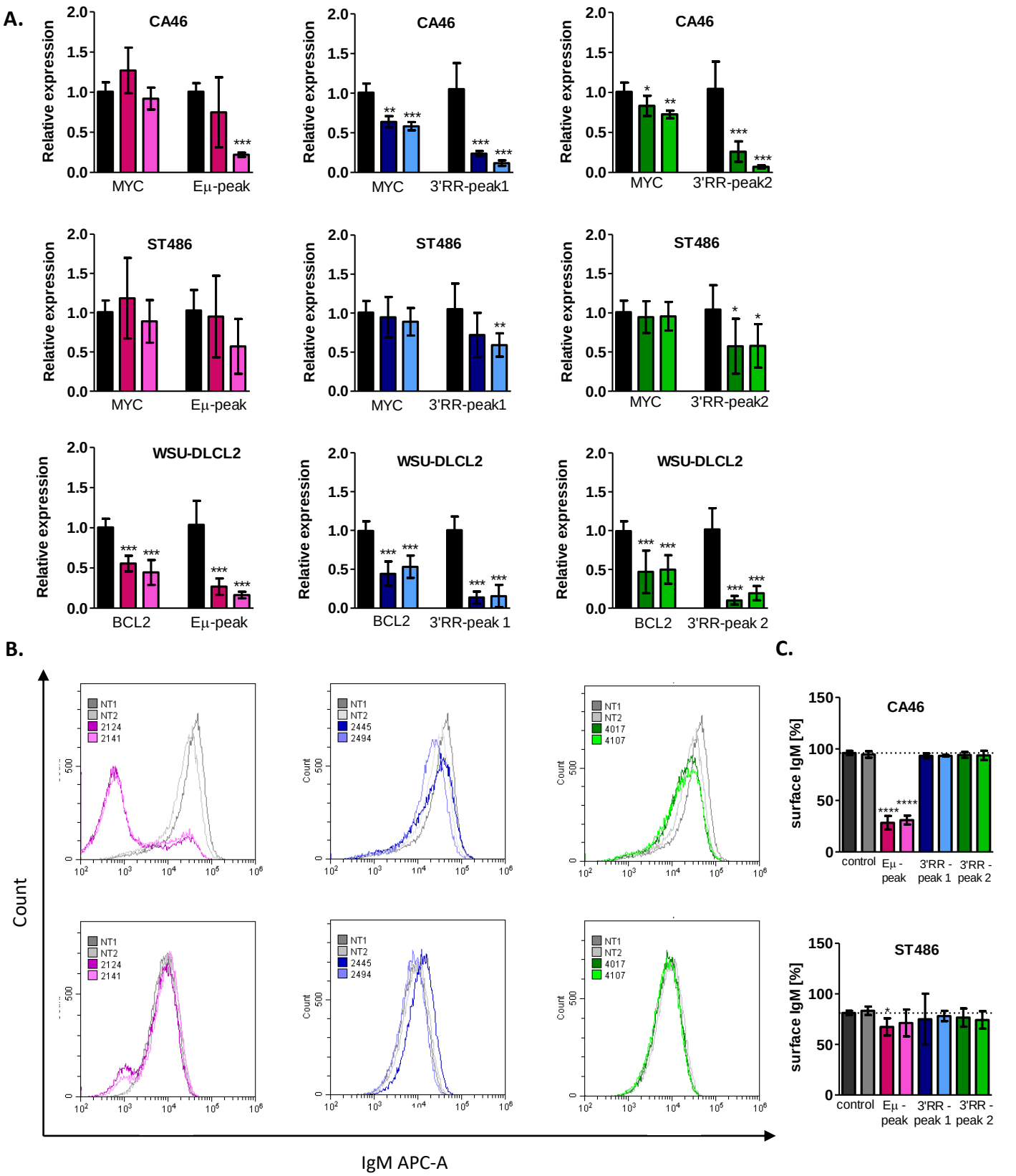

Figure 6. Downstream effects of targeting *IGH* enhancers. A. Expression of oncogenes involved in *IGH* translocation – MYC (CA46, ST486) or BCL2 (WSU-DLCL2) and expression of eRNAs upon blocking of *IGH* enhancers essential regions on RNA level determined by qRT-PCR. Mean and SD of three independent biological replicates is shown. Expression normalized to HPRT. *, P ≤ 0.05; **, P ≤ 0.01, ***, P ≤ 0.001, Mann-Whitney test. **B.** Immunostaining of B-cell receptor (BCR) on cell surface CA46 and ST486 (IgM) (WSU-DLCL2 do not express neither IgM nor IgG). Representative histograms of overlaid data for non-targeting controls (grey) and sgRNAs targeting *IGH*-enhancers essential regions (pink, Eμ peak; blue, 3'RR peak 1; green, 3'RR peak 2). **C.** Average and SD of percentage of BCR-positive cells (surface IgM) from two biological replicates. *, P ≤ 0.05; **, P ≤ 0.01; ***, P ≤ 0.001; ****, P ≤ 0.0001, Student's two-tailed t-test.

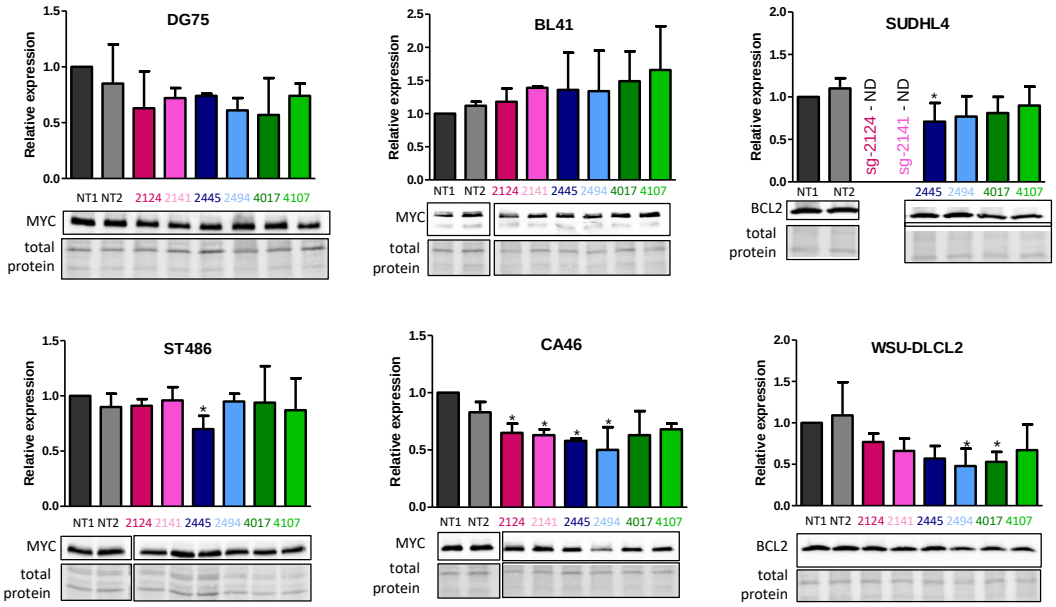

Supplementary Figure 7. Expression of oncogenes (MYC or BCL2) on protein level. Mean and SD from two independent biological replicates is shown. Protein bands were normalized to the total protein. ND – not determined due to insufficient cell number.

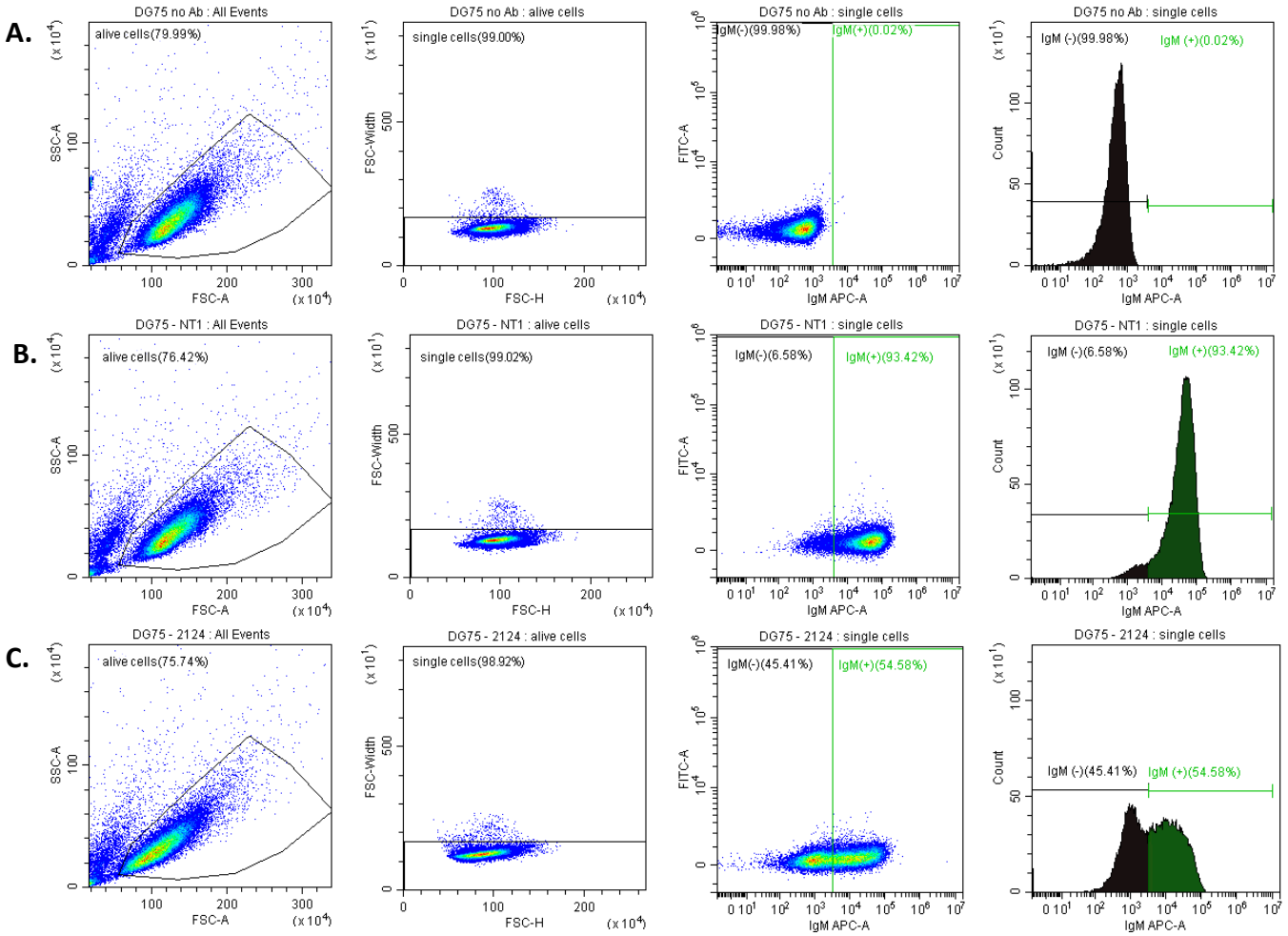

Supplementary Figure 8. Flow cytometry analysis of B-cell receptor (BCR) immunostaining. APC-based gating strategy for surface BCR analysis, from left: living cells selection, single cells selection, surface BCR positive (IgM or IgG) cells selection and histogram visualization. Examples are given for **A.** sample without anti-BCR antibody, **B.** control sample NT1, **C.** sample in which Eμ enhancer is targeted with sgRNA

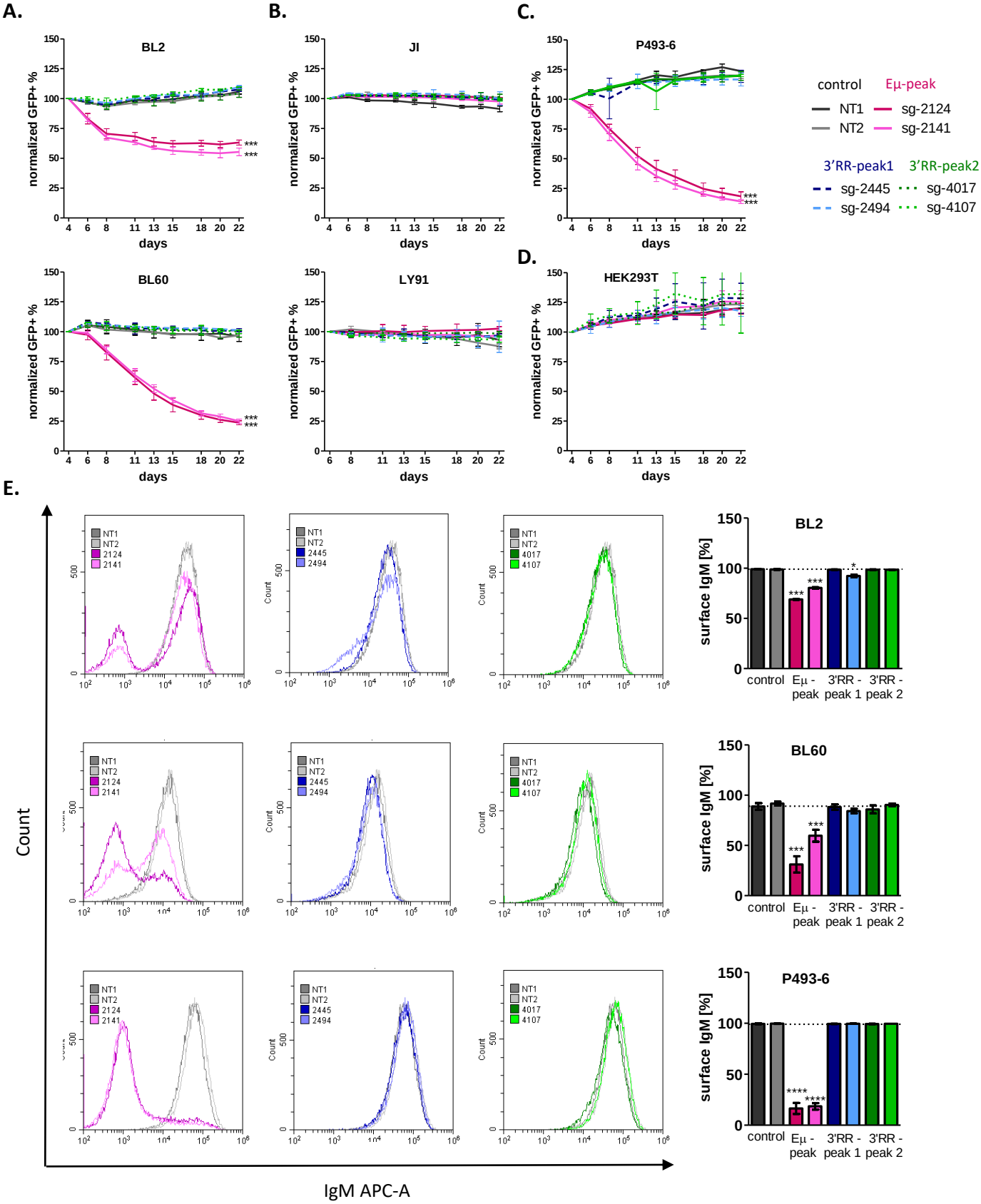

Supplementary Figure 9. Effect of targeting IGH enhancers in cells without IGH translocations. A-D. GFP growth competition assay in **A.** BL cell lines with MYC-IGL t(8;22) translocation (BL2, BL60); **B.** BL cell lines with MYC-IGK t(2;8) translocation (JI, LY91); **C.** B-cell cell line without MYC translocation (P493-6); **D.** Embryonic kidney HEK293T cell line. Assay performed with individual sgRNAs over the course of 3 weeks. Average and standard deviation from 2-3 independent biological replicates is shown. ***, P≤0.001, mixed model analysis. **E.** Immunostaining of B-cell receptor (BCR) on cell surface in BL2, BL60 and P4936 cells (all IgM, JI and LY91 are BCR-negative). Representative histograms of overlaid data for non-targeting controls (grey) and sgRNAs targeting *IGH*-enhancers essential regions (pink, Eμ peak; blue, 3'RR peak 1; green, 3'RR peak 2). Column graphs show average percentage and SD of BCR-positive cells (surface IgM) from two biological replicates. *, P ≤ 0.05; ***, P ≤ 0.001; ****, P ≤ 0.0001, Student's two-tailed t-test.

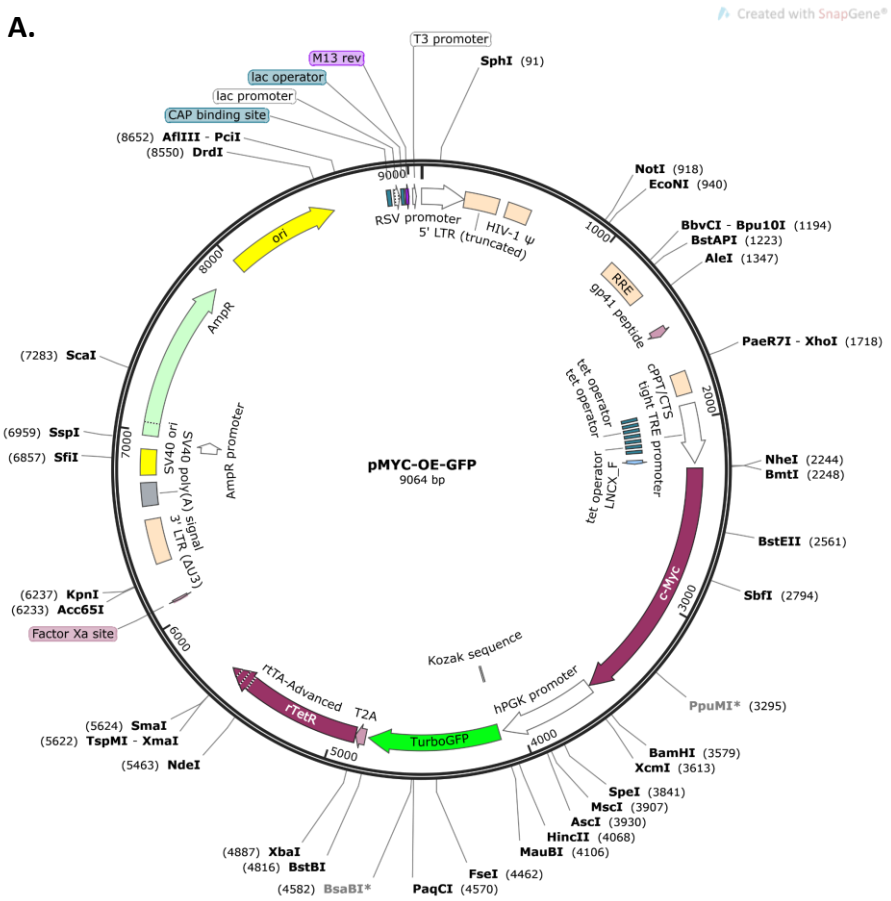

Supplementary Figure 10. Establishment of MYC-overexpressing DG75 cells. A. Map of plasmid pMYC-OE-GFP used for establishment of DG75-MYC-OE cell line. **B-C.** Validation of doxycycline-induced MYC overexpression in DG75- MYC-OE cell line on **B.** RNA level, expression normalized to HPRT and **C.** on protein level, normalized to total protein. **D.** DG75-MYC-OE cells (expressing GFP) survival upon doxycycline-induced MYC overexpression over 3 weeks of culture determined by GFP growth competition assay.

Supplementary Table 4. List of primers used in this study.

Name	Sequence - Fwd 5'-3’	Sequence - Rev 5'-3’
Gene expression analysis		
HPRT	GGCAGTATAATCCAAAGATGGTCAA	GTCTGGCTTATATCCAACACTTCGT
TBP	GCCCGAAACGCCGAATAT	CCGTGGTTCGTGGCTCTCT
GAPDH	GAGTCCACTGGCGTCTTCAC	TGATGACCCTTTTGGCTCCC
Eμ-peak	TCCTACAGACACCGCTCCTG	GGCTTGGGGAGCCACATTT
3'RR peak 1	TGACCCCCGATGAGTGTGAG	TGGATAACGCTCAGGACGGG
3'RR peak 2	GCCCAGAGATGCCGAAAACT	CTAGGGGCAAGCTGGTGAG
MYC	CACCAGCAGCGACTCTGA	ATCCAGACTCTGACCTTTTGC
BCL2	TGAACTGGGGGAGGATTGTG	CGTACAGTTCCACAAAGGCA
TBP_intron	TTTGTCTGAAGCCCTGATGTGT	CTGTGAAGAGAGCGCAGTGT
GAPDH_exon-intron	AATCCCATCACCATCTTCCAG	GAGCCACACCATCCTAGTTG
Fractionation controls		
TBP_intron	TTTGTCTGAAGCCCTGATGTGT	CTGTGAAGAGAGCGCAGTGT
KTN1_AS1_intron	TTGGCTGCTATTTACTACCCTCC	GCTGGGTGTGTTGCTAATCC
RPPH1	AGCTTGGAACAGACTCACGG	AATGGGCGGAGGAGAGTAGT
DANCR	CGTCTCTTACGTCTGCGGAA	TGGCTTGTGCCTGTAGTTGT
U3 snoRNA	AACCCCGAGGAAGAGAGGTA	CACTCCCCAATACGGAGAGA
MIAT	TGGAGGCATCTGTCCACCCATGT	CCCTGTGATGCCGACGGGGT
CRISPR-eIGH library amplification		
oligo-F/R	GTAACTTGAAAGTATTTCGATTTCTTGGCTTTA TATATCTTGTGGAAAGGACGAAACACC	ACTTTTTCAAGTTGATAACGGACTAGCCTTAT TTTAACTTGCTATTTCTAGCTCTAAAAC

Supplementary Table 5. List of sgRNA oligonucleotides used in CRISPRi screens validation. Bold– overhangs for cloning.

Name	Target region	Sequence - Sense 5'-3'	Sequence - Antisens 5'-3'
sg-2124	Eμ peak	**CACCG**TCCCTAAGCCCCTGTCAGGA	**AAAC**TCCTGACAGGGGCTTAGGGA**C**
sg-2141	Eμ peak	**CACCG**CCCTGCTCTCATCAAGACCG	**AAAC**CGGTCTTGATGAGAGCAGGG**C**
sg-2445	3'RR_peak 1	**CACCG**TGGGGGGAAGGCTGGCACCC	**AAAC**GGGTGCCAGCCTTCCCCCCA**C**
sg-2494	3'RR_peak 1	**CACCG**GCTGCGGCCCGGTGCCCATG	**AAAC**CATGGGCACCGGGCCGCAGC**C**
sg-4017	3'RR_peak 2	**CACCG**TGACTCATTCTGGGCAGACT	**AAAC**AGTCTGCCCAGAATGAGTCA**C**
sg-4107	3'RR_peak 2	**CACCG**CCCGAGGCTAGGCTGTGGGA	**AAAC**TCCCACAGCCTAGCCTCGGG**C**
sg-NT1	non-targeting control	**CACCG**ACGGAGGCTAAGCGTCGCAA	**AAAC**TTGCGACGCTTAGCCTCCGT**C**
sg-NT2	non-targeting control	**CACCG**ATCGTTTCCGCTTAACGGCG	**AAAC**CGCCGTTAAGCGGAAACGAT**C**

Supplementary Table 6. List of primers used in preparation of CRISPR-eIGH library for NGS.

Name	Sequence 5'-3'
Fwd-1	AATGATACGGCGACCACCGAGATCTACACTCTTTCCCTACACGACGCTCTTCCGATCTTAAGTAGAGGCTTTATATATCTTGTGGAAAGGACGAAACACC
Fwd-2	AATGATACGGCGACCACCGAGATCTACACTCTTTCCCTACACGACGCTCTTCCGATCTATCATGCTTAGCTTTATATATCTTGTGGAAAGGACGAAACACC
Fwd-3	AATGATACGGCGACCACCGAGATCTACACTCTTTCCCTACACGACGCTCTTCCGATCTGATGCACATCTGCTTTATATATCTTGTGGAAAGGACGAAACACC
Fwd-4	AATGATACGGCGACCACCGAGATCTACACTCTTTCCCTACACGACGCTCTTCCGATCTCGATTGCTCGACGCTTTATATATCTTGTGGAAAGGACGAAACACC
Fwd-5	AATGATACGGCGACCACCGAGATCTACACTCTTTCCCTACACGACGCTCTTCCGATCTTCGATAGCAATTCGCTTTATATATCTTGTGGAAAGGACGAAACACC
Fwd-6	AATGATACGGCGACCACCGAGATCTACACTCTTTCCCTACACGACGCTCTTCCGATCTATCGATAGTTGCTTGCTTTATATATCTTGTGGAAAGGACGAAACACC
Fwd-7	AATGATACGGCGACCACCGAGATCTACACTCTTTCCCTACACGACGCTCTTCCGATCTGATCGATCCAGTTAGGCTTTATATATCTTGTGGAAAGGACGAAACACC
Fwd-8	AATGATACGGCGACCACCGAGATCTACACTCTTTCCCTACACGACGCTCTTCCGATCTCGATCGATTTGAGCCTGCTTTATATATCTTGTGGAAAGGACGAAACACC
Fwd-9	AATGATACGGCGACCACCGAGATCTACACTCTTTCCCTACACGACGCTCTTCCGATCTACGATCGATACACGATCGCTTTATATATCTTGTGGAAAGGACGAAACACC
Fwd-10	AATGATACGGCGACCACCGAGATCTACACTCTTTCCCTACACGACGCTCTTCCGATCTTACGATCGATGGTCCAGAGCTTTATATATCTTGTGGAAAGGACGAAACACC
Rev-1	CAAGCAGAAGACGGCATACGAGATTCGCCTTGGTGACTGGAGTTCAGACGTGTGCTCTTCCGATCTCCGACTCGGTGCCACTTTTTCAA
Rev-2	CAAGCAGAAGACGGCATACGAGATATAGCGTCGTGACTGGAGTTCAGACGTGTGCTCTTCCGATCTCCGACTCGGTGCCACTTTTTCAA
Rev-3	CAAGCAGAAGACGGCATACGAGATGAAGAAGTGTGACTGGAGTTCAGACGTGTGCTCTTCCGATCTCCGACTCGGTGCCACTTTTTCAA
Rev-4	CAAGCAGAAGACGGCATACGAGATATTCTAGGGTGACTGGAGTTCAGACGTGTGCTCTTCCGATCTCCGACTCGGTGCCACTTTTTCAA
Rev-5	CAAGCAGAAGACGGCATACGAGATCGTTACCAGTGACTGGAGTTCAGACGTGTGCTCTTCCGATCTCCGACTCGGTGCCACTTTTTCAA
Rev-6	CAAGCAGAAGACGGCATACGAGATGTCTGATGGTGACTGGAGTTCAGACGTGTGCTCTTCCGATCTCCGACTCGGTGCCACTTTTTCAA
Rev-7	CAAGCAGAAGACGGCATACGAGATTTACGCACGTGACTGGAGTTCAGACGTGTGCTCTTCCGATCTCCGACTCGGTGCCACTTTTTCAA
Rev-8	CAAGCAGAAGACGGCATACGAGATTTGAATAGGTGACTGGAGTTCAGACGTGTGCTCTTCCGATCTCCGACTCGGTGCCACTTTTTCAA

Supplementary Table 7. List of antibodies used in this study. WB – Western Blot; IC – Immunostaining.

Name	Host species	Company	Catalog number	Amount / dliution used	Purpose
Primary Antibodies					
Cellular Fractionation					
H3	Rabbit	Abcam	ab18521	1:1000	WB
Beta tubulin	Mouse	Abcam	ab131205	1:5000	WB
U1 snRNP 70	Mouse	Santa Cruz Biotechnology	sc-390899	1:500	WB
dCas9 expression validation					
Cas9	Mouse	Cell Signaling	#14697	1:1000	WB
Oncogene expression					
Bcl2	Rabbit	Abcam	ab32124	1:5000	WB; SU-DHL-4
Bcl2	Mouse	BD Biosciences	610538	1:1000	WB; WSU-DLCL2
Myc	Rabbit	Abcam	ab32072	1:10 000	WB
BCR immunostaining					
IgG	Goat	Sothern Biotech	2042-31	0.1 µg	IC
IgM	Mouse	BD Biosciences	551062	20 µl	IC
Secondary Antibodies					
Anti-Mouse	Goat	Santa Cruz Biotechnology	sc-2005	1:10 000	WB
Anti-Rabbit	Goat	Abcam	ab6721	1:5000	WB